1 Title Page

Bimodal Inference in Humans and Mice

Authors:

Veith Weilnhammer[1,2], Heiner Stuke[1,2], Kai Standvoss[1,3,5], Philipp Sterzer[6]

Affiliations:

[1] Department of Psychiatry, Charité-Universitätsmedizin Berlin, corporate member of Freie Universität Berlin and Humboldt-Universität zu Berlin, 10117 Berlin, Germany

[2] Berlin Institute of Health, Charité-Universitätsmedizin Berlin and Max Delbrück Center, 10178 Berlin, Germany

[3] Bernstein Center for Computational Neuroscience, Charité-Universitätsmedizin Berlin, 10117 Berlin, Germany

[4] Berlin School of Mind and Brain, Humboldt-Universität zu Berlin, 10099 Berlin, Germany

[5] Einstein Center for Neurosciences Berlin, 10117 Berlin, Germany

[6] Department of Psychiatry (UPK), University of Basel, Switzerland

Corresponding Author:

Veith Weilnhammer, Department of Psychiatry, Charité Campus Mitte, Charitéplatz 1, 10117 Berlin, phone: 0049 (0)30 450 517 317, email: veith.weilnhammer@gmail.com

2 Abstract

Perception is known to cycle through periods of enhanced and reduced sensitivity to external information. Here, we asked whether such slow fluctuations arise as a noise-related epiphenomenon of limited processing capacity or, alternatively, represent a structured mechanism of perceptual inference. Using two large-scale datasets, we found that humans and mice alternate between externally- and internally-oriented modes of sensory analysis. During external mode, perception aligns more closely with the external sensory information, whereas internal mode is characterized by enhanced biases toward perceptual history. Computational modeling indicated that dynamic changes in mode are enabled by two interlinked factors: (i), the integration of subsequent inputs over time and, (ii), slow anti-phase oscillations in the perceptual impact of external sensory information versus internal predictions that are provided by perceptual history. We propose that between-mode fluctuations generate unambiguous error signals that enable optimal inference in volatile environments.

3 One sentence summary

Humans and mice fluctuate between external and internal modes of sensory processing.

4 Introduction

The capacity to respond to changes in the environment is a defining feature of life[1–3]. Intriguingly, the ability of living things to process their surroundings fluctuates considerably over time[4,5]. In humans and mice, perception[6–12], cognition[13] and memory[14] cycle through prolonged periods of enhanced and reduced sensitivity to external information, suggesting that the brain detaches from the world in recurring intervals that last from milliseconds to seconds and even minutes[4]. Yet breaking from external information is risky, as swift responses to the environment are often crucial to survival.

What could be the reason for these fluctuations in perceptual performance[11]? First, periodic fluctuations in the ability to parse external information[11,15,16] may arise simply due to bandwidth limitations and noise. Second, it may be advantageous to actively reduce the costs of neural processing by seeking sensory information only in recurring intervals[17], otherwise relying on random or stereotypical responses to the external world. Third, spending time away from the ongoing stream of sensory inputs may also reflect a functional strategy that facilitates flexible behavior and learning[18]: Intermittently relying more strongly on information acquired from past experiences may enable agents to build up stable internal predictions about the environment despite an ongoing stream of external sensory signals[19]. By the same token, recurring intervals of enhanced sensitivity to external information may help to detect changes in both the state of the environment and the amount of noise that is inherent in sensory encoding[19].

In this work, we sought to elucidate whether periodicities in the sensitivity to external information represent an epiphenomenon of limited processing capacity or, alternatively, result from a structured and adaptive mechanism of perceptual inference. To this end, we analyzed two large-scale datasets on perceptual decision-making in humans[20] and mice[21]. When less sensitive to external stimulus information, humans and mice did not behave more randomly, but showed stronger serial dependencies in their perceptual choices[22–33]. These

serial dependencies may be understood as driven by internal predictions that reflect the auto-correlation of natural environments[34] and bias perception toward preceding experiences[30,31,35]. Computational modeling indicated that ongoing changes in perceptual performance may be driven by systematic fluctuations between externally- and internally-oriented *modes* of sensory analysis. We suggest that such *bimodal inference* may help to build stable internal representations of the sensory environment despite an ongoing stream of sensory information.

5 Results

5.1 Human perception fluctuates between epochs of enhanced and reduced sensitivity to external information

We began by selecting 66 studies from the Confidence Database[20] that investigated how human participants (N = 4317) perform binary perceptual decisions (Figure 1A; see Methods for details on inclusion criteria). As a metric for perceptual performance (i.e., the sensitivity to external sensory information), we asked whether the participant's response and the presented stimulus matched (*stimulus-congruent* choices) or differed from each other (*stimulus-incongruent* choices; Figure 1B and C) in a total of 21.05 million trials.

In a first step, we asked whether the ability to accurately perceive sensory stimuli is constant over time or, alternatively, fluctuates in periods of enhanced and reduced sensitivity to external information. We found perception to be stimulus-congruent in 73.46% ± 0.15% of trials (mean ± standard error of the mean; Figure 2A), which was highly consistent across the selected studies (Supplemental Figure S1A). In line with previous work[8], we found that the probability of stimulus-congruence was not independent across successive trials: At the group level, stimulus-congruent perceptual choices were significantly autocorrelated for up to 15 trials (Figure 2B), controlling for task difficulty and the sequence of presented stimuli (Supplemental Figure 2A-B).

At the level of individual participants, the autocorrelation of stimulus-congruence exceeded the respective autocorrelation of randomly permuted data within an interval of $3.24 \pm 2.39 \times 10^{-3}$ trials (Figure 2C). In other words, if a participant's experience was congruent (or incongruent) with the external stimulus information at a given trial, her perception was more likely to remain stimulus-congruent (or -incongruent) for approximately 3 trials into the future. The autocorrelation of stimulus-congruence was corroborated by logistic regression models that successfully predicted the stimulus-congruence of perception at the index trial $t = 0$ from the stimulus-congruence at the preceding trials within a lag of 16 trials (Supplemental Figure S3).

These results confirm that the ability to process sensory signals is not constant over time but unfolds in multi-trial epochs of enhanced and reduced sensitivity to external information[8]. As a consequence of this autocorrelation, the dynamic probability of stimulus-congruent perception (i.e., computed in sliding windows of $\pm$ 5 trials; Figure 1C) fluctuated considerably within participants (average minimum: 35.46% $\pm$ 0.22%, maximum: 98.27% $\pm$ 0.07%). In line with previous findings[9], such fluctuations in the sensitivity to external information had a power density that was inversely proportional to the frequency in the slow spectrum[11] (power $\sim 1/f^{\beta}$, $\beta = -1.32 \pm 3.14 \times 10^{-3}$, $\mathrm{T}(1.84 \times 10^{5}) = -419.48$, $\mathrm{p} < 2.2 \times 10^{-308}$; Figure 2D). This feature, which is also known as a *1/f power law*[36,37], represents a characteristic of scale-free fluctuations in complex dynamic systems such as the brain[38] and the cognitive processes it entertains[9,10,13,39,40].

5.2 Humans fluctuate between external and internal modes of sensory processing

In a second step, we sought to explain why perception cycles through periods of enhanced and reduced sensitivity to external information[4]. We reasoned that observers may intermittently rely more strongly on internal information, i.e., on predictions about the environment that

are constructed from previous experiences[19,31].

In perception, *serial dependencies* represent one of the most basic internal predictions that cause perceptual decisions to be systematically biased toward preceding choices[22–33]. Such effects of perceptual history mirror the continuity of the external world, in which the recent past often predicts the near future[30,31,34,35,41]. Therefore, as a metric for the perceptual impact of internal information, we computed whether the participant's response at a given trial matched or differed from her response at the preceding trial (*history-congruent* and *history-incongruent perception*, respectively; Figure 1B and C).

First, we confirmed that perceptual history played a significant role in perception despite the ongoing stream of external information. With a global average of 52.7% ± 0.12% history-congruent trials, we found a small but highly significant perceptual bias towards preceding experiences ($\beta = 16.18 \pm 1.07$, $T(1.09 \times 10^3) = 15.07$, $p = 10^{-46}$; Figure 2A) that was largely consistent across studies (Supplemental Figure 1B) and more pronounced in participants who were less sensitive to external sensory information (Supplemental Figure 1C). Importantly, history-congruence was not a corollary of the sequence of presented stimuli: History-congruent perceptual choices were more frequent at trials when perception was stimulus-incongruent (56.03% ± 0.2%) as opposed to stimulus-congruent (51.77% ± 0.11%, $\beta = -4.26 \pm 0.21$, $T(8.57 \times 10^3) = -20.36$, $p = 5.28 \times 10^{-90}$; Figure 2A, lower panel). Despite being adaptive in autocorrelated real-world environments[19,34,35,42], perceptual history thus represented a source of bias in the randomized experimental designs studied here[24,28,30,31,43]. These serial biases were effects of choice history, i.e., driven by the experiences reported at the preceding trial, and could not be attributed to stimulus history, i.e., to effects of the stimuli presented at the preceding trial (Supplemental Section 9.1).

Second, we asked whether perception cycles through multi-trial epochs during which perception is characterized by stronger or weaker biases toward preceding experiences. In close analogy to stimulus-congruence, we found history-congruence to be significantly autocorrelated for up

to 21 trials (Figure 2B), while controlling for task difficulty and the sequence of presented stimuli (Supplemental Figure 2A-B). In individual participants, the autocorrelation of history-congruence was elevated above randomly permuted data for a lag of $4.87 \pm 3.36 \times 10^{-3}$ trials (Figure 2C), confirming that the autocorrelation of history-congruence was not only a group-level phenomenon. The autocorrelation of history-congruence was corroborated by logistic regression models that successfully predicted the history-congruence of perception at an index trial $t = 0$ from the history-congruence at the preceding trials within a lag of 17 trials (Supplemental Figure S3).

Third, we asked whether the impact of internal information fluctuates as a scale-invariant process with a 1/f power law (i.e., the feature typically associated with fluctuations in the sensitivity to external information[9,10,13,39,40]). The dynamic probability of history-congruent perception (i.e., computed in sliding windows of ± 5 trials; Figure 1C) varied considerably over time, ranging between a minimum of 12.77% ± 0.14% and a maximum 92.23% ± 0.14%. In analogy to stimulus-congruence, we found that history-congruence fluctuated as at power densities that were inversely proportional to the frequency in the slow spectrum[11] (power ~ $1/f^{\beta}$, $\beta = -1.34 \pm 3.16 \times 10^{-3}$, $T(1.84 \times 10^5) = -423.91$, $p < 2.2 \times 10^{-308}$; Figure 2D).

Finally, we ensured that fluctuations in stimulus- and history-congruence are linked to each other. When perceptual choices were less biased toward external information, participants relied more strongly on internal information acquired from perceptual history (and vice versa, $\beta = -0.05 \pm 5.63 \times 10^{-4}$, $T(2.1 \times 10^6) = -84.21$, $p < 2.2 \times 10^{-308}$, controlling for fluctuations in general response biases; Supplemental Section 9.2). Thus, while sharing the 1/f power law characteristic, fluctuations in stimulus- and history-congruence were shifted against each other by approximately half a cycle and showed a squared coherence of $6.49 \pm 2.07 \times 10^{-3}$% (Figure 2E and F; we report the average phase and coherence for frequencies below 0.1 $1/N_{trials}$; see Methods for details).

In sum, our analyses indicate that perceptual decisions may result from a competition between

external sensory signals with internal predictions provided by perceptual history. We show that the impact of these external and internal sources of information is not stable over time, but fluctuates systematically, emitting overlapping autocorrelation curves and antiphase 1/f profiles.

These links between stimulus- and history-congruence suggest that the fluctuations in the impact of external and internal information may be generated by a unifying mechanism that causes perception to alternate between two opposing *modes*[18] (Figure 1D): During *external mode*, perception is more strongly driven by the available external stimulus information. Conversely, during *internal mode*, participants rely more heavily on internal predictions that are implicitly provided by preceding perceptual experiences. The fluctuations in the degree of bias toward external versus internal information created by such *bimodal inference* may thus provide a novel explanation for ongoing fluctuations in the sensitivity to external information[4,5,18].

5.3 Internal and external modes of processing facilitate response behavior and enhance confidence in human perceptual decision-making

The above results point to systematic fluctuations in the *decision variable*[44] that determines perceptual choices, causing enhanced sensitivity to external stimulus information during external mode and increased biases toward preceding choices during internal mode. As such, fluctuations in mode should influence downstream aspects of behavior and cognition that operate on the perceptual decision variable[44]. To test this hypothesis with respect to motor behavior and metacognition, we asked how bimodal inference relates to response times (RTs) and confidence reports.

With respect to RTs, we observed faster responses for stimulus-congruent as opposed to stimulus-incongruent choices ($\beta = -0.14 \pm 1.6\times10^{-3}$, $T(1.99\times10^{6}) = -85.84$, $p < 2.2\times10^{-308}$;

Figure 2G). Intriguingly, whilst controlling for the effect of stimulus-congruence, we found that history-congruent (as opposed to history-incongruent) choices were also characterized by faster responses ($\beta = -9.56 \times 10^{-3} \pm 1.37 \times 10^{-3}$, $T(1.98 \times 10^6) = -6.97$, $p = 3.15 \times 10^{-12}$; Figure 2G).

When analyzing the speed of response against the mode of sensory processing (Figure 2H), we found that RTs were shorter during externally-oriented perception ($\beta_1 = -11.07 \pm 0.55$, $T(1.98 \times 10^6) = -20.14$, $p = 3.17 \times 10^{-90}$). Crucially, as indicated by a quadratic relationship between the mode of sensory processing and RTs ($\beta_2 = -19.86 \pm 0.52$, $T(1.98 \times 10^6) = -38.43$, $p = 5 \times 10^{-323}$), participants became faster at indicating their perceptual decision when biases toward both internal and external mode grew stronger.

In analogy to the speed of response, confidence was higher for stimulus-congruent as opposed to stimulus-incongruent choices ($\beta = 0.04 \pm 1.18 \times 10^{-3}$, $T(2.06 \times 10^6) = 36.85$, $p = 3.25 \times 10^{-297}$; Figure 2I). Yet whilst controlling for the effect of stimulus-congruence, we found that history-congruence also increased confidence ($\beta = 0.48 \pm 1.38 \times 10^{-3}$, $T(2.06 \times 10^6) = 351.54$, $p < 2.2 \times 10^{-308}$; Figure 2I).

When depicted against the mode of sensory processing (Figure 2J), subjective confidence was indeed enhanced when perception was more externally-oriented ($\beta_1 = 92.63 \pm 1$, $T(2.06 \times 10^6) = 92.89$, $p < 2.2 \times 10^{-308}$). Importantly, however, participants were more confident in their perceptual decision for stronger biases toward both internal and external mode ($\beta_2 = 39.3 \pm 0.94$, $T(2.06 \times 10^6) = 41.95$, $p < 2.2 \times 10^{-308}$). In analogy to RTs, subjective confidence thus showed a quadratic relationship to the mode of sensory processing (Figure 2J).

Consequently, our findings predict that human participants lack full metacognitive insight into how strongly external signals and internal predictions contribute to perceptual decision-making. Stronger biases toward perceptual history thus lead to two seemingly contradictory effects, more frequent errors (Supplemental Figure 1C) and increasing subjective confidence (Figure 2I-J). This observation generates an intriguing prediction regarding the association of

between-mode fluctuations and perceptual metacognition: Metacognitive efficiency should be lower in individuals who spend more time in internal mode, since their confidence reports are less predictive of whether the corresponding perceptual decision is correct. We computed each participant's M-ratio[45] (meta-d'/d' = 0.85 ± 0.02) to probe this hypothesis independently of inter-individual differences in perceptual performance. Indeed, we found that biases toward internal information (as defined by the average probability of history-congruence) were stronger in participants with lower metacognitive efficiency ($\beta = -2.98 \times 10^{-3} \pm 9.82 \times 10^{-4}$, $T(4.14 \times 10^3) = -3.03$, $p = 2.43 \times 10^{-3}$).

In sum, the above results indicate that reporting behavior and metacognition do not map linearly onto the mode of sensory processing. Rather, they suggest that slow fluctuations in the respective impact of external and internal information are most likely to affect perception at an early level of sensory analysis[46,47]. Such low-level processing may thus integrate perceptual history with external inputs into a decision variable[44] that influences not only perceptual choices, but also the speed and confidence at which they are made.

In what follows, we probe alternative explanations for between-mode fluctuations, test for the existence of modes in mice, and propose a predictive processing model that explains fluctuations in mode ongoing shifts in the precision afforded to external sensory information relative to internal predictions driven by perceptual history.

5.4 Fluctuations between internal and external mode cannot be reduced to general response biases or random choices

The core assumption of bimodal inference - that ongoing changes in the sensitivity to external information are driven by internal predictions induced via perceptual history - needs to be contrasted against two alternative hypotheses: When making errors, observers may not engage with the task and respond stereotypically, i.e., exhibit stronger general biases toward one of the two potential outcomes, or simply choose randomly.

Logistic regression confirmed that perceptual history made a significant contribution to perception ($\beta = 0.11 \pm 5.79 \times 10^{-3}$, z = 18.53, p = 1.1×10^{-76}) over and above the ongoing stream of external sensory information ($\beta = 2.2 \pm 5.87 \times 10^{-3}$, z = 375.11, p < 2.2×10^{-308}) and general response biases toward ($\beta = 15.19 \pm 0.08$, z = 184.98, p < 2.2×10^{-308}).

When eliminating perceptual history as a predictor of individual choices at individual trials, Akaike Information Criterion (AIC[48]) increased by $\delta_{AIC} = 1.64 \times 10^3$ (see Supplemental Figure S4A-B for parameter- and model-level inference at the level of individual observers). Likewise, when eliminating slow fluctuations in history-congruence as a predictor of slow fluctuations in stimulus-congruence across trials, we observed an increase in AIC by $\delta_{AIC} = 7.06 \times 10^3$. These results provided model-level evidence against the null hypotheses that fluctuations in stimulus-congruence are driven exclusively by choice randomness or general response bias (see Supplemental Section 9.2 and Supplemental Figure S5 for an in-depth assessment of general response bias).

To confirm that changes in the sensitivity to external information are indicative of internal mode processing, we estimated full and history-dependent psychometric curves during internal, external, and across modes[21]. If, as we hypothesized, internal mode processing reflects an enhanced impact of perceptual history, one would expect a history-dependent increase in biases and lapses as well as a history-independent increase in threshold. Conversely, if internal mode processing were driven by random choices, one would expect a history-independent increase in lapses and threshold, and no change in bias. In line with our prediction, we found that internal mode processing was associated with a history-dependent increase in bias and lapse as well as a history-independent increase in threshold (Supplemental Section 9.3.1 and Supplemental Figure S6). This confirmed that internal mode processing is indeed driven by an enhanced impact of perceptual history.

In line with this, the quadratic relationship between mode and confidence (Figure 2J) suggested that biases toward internal information do not reflect a post-perceptual strategy

of repeating preceding choices when the subjective confidence in the perceptual decision is low. Moreover, while responses became faster with longer exposure to the experiments of the Confidence database, the frequency of history-congruent choices increased over time, speaking against the proposition that participants stereotypically repeat preceding choices when not yet familiar with the experimental task (Supplemental Section 9.4.1).

Taken together, our results thus argue against recurring intervals of low task engagement, which may be signaled by stereotypical or random responses, as an alternative explanation for the phenomenon that we identify as bimodal inference.

5.5 Mice fluctuate between external and internal modes of sensory processing

In a prominent functional explanation for serial dependencies[22–28,32,33,46], perceptual history is cast as an internal prediction that leverages the temporal autocorrelation of natural environments for efficient decision-making[30,31,34,35,41]. Since this autocorrelation is one of the most basic features of our sensory world, fluctuating biases toward preceding perceptual choices should not be a uniquely human phenomenon.

To test whether externally- and internally-oriented modes of processing exist beyond the human mind, we analyzed data on perceptual decision-making in mice that were extracted from the International Brain Laboratory (IBL) dataset[21]. We restricted our analyses to the *basic* task[21], in which mice responded to gratings of varying contrast that appeared either in the left or right hemifield of with equal probability. We excluded sessions in which mice did not respond correctly to stimuli presented at a contrast above 50% in more than 80% of trials (see Methods for details), which yielded a final sample of N = 165 adequately trained mice that went through 1.46 million trials.

We found perception to be stimulus-congruent in 81.37% ± 0.3% of trials (Figure 3A, upper panel). In line with humans, mice were biased toward perceptual history in 54.03% ± 0.17%

of trials ($T(164) = 23.65$, $p = 9.98 \times 10^{-55}$; Figure 3A and Supplemental Figure S1D). Since the *basic* task of the IBL dataset presented stimuli at random in either the left or right hemifield[21], we expected stronger biases toward perceptual history to decrease perceptual performance. Indeed, history-congruent choices were more frequent when perception was stimulus-incongruent ($61.59\% \pm 0.07\%$) as opposed to stimulus-congruent ($51.81\% \pm 0.02\%$, $T(164) = 31.37$, $p = 3.36 \times 10^{-71}$; $T(164) = 31.37$, $p = 3.36 \times 10^{-71}$; Figure 3A, lower panel), confirming that perceptual history was a source of bias[24,28,30,31,43] as opposed to a feature of the experimental paradigm.

At the group level, we found significant autocorrelations in both stimulus-congruence (42 consecutive trials) and history-congruence (8 consecutive trials; Figure 3B), while controlling for the respective autocorrelation of task difficulty and external stimulation (Supplemental Figure 2C-D). In contrast to humans, mice showed a negative autocorrelation coefficient of stimulus-congruence at trial 2, which was due to a feature of the experimental design: Errors at a contrast above 50% were followed by a high-contrast stimulus at the same location. Thus, stimulus-incongruent choices on easy trials were more likely to be followed by stimulus-congruent perceptual choices that were facilitated by high-contrast visual stimuli[21].

At the level of individual mice, autocorrelation coefficients were elevated above randomly permuted data within a lag of 4.59 ± 0.06 trials for stimulus-congruence and 2.58 ± 0.01 trials for history-congruence (Figure 3C). We corroborated these autocorrelations in logistic regression models that successfully predicted the stimulus-/history-congruence of perception at the index trial $t = 0$ from the stimulus-/history-congruence at the 33 preceding trials for stimulus-congruence and 8 preceding trials for history-congruence (Supplemental Figure S3). In analogy to humans, mice showed anti-phase 1/f fluctuations in the sensitivity to internal and external information (Figure 3D-F).

The above results confirm that fluctuations between internally- and externally-biased modes generalize to perceptual decision-making in mice. Following our hypothesis that bimodal

inference operates at the level of perception, we predicted that between-mode fluctuations modulate a decision variable[44] that determines not only perceptual choices, but also downstream aspects of mouse behavior[44]. We therefore asked how external and internal modes relate to the trial duration (TD, a coarse measure of RT in mice that spans the interval from stimulus onset to feedback[21]). Stimulus-congruent (as opposed to stimulus-incongruent) choices were associated with shorter TDs ($\delta = -262.48 \pm 17.1$, T(164) = -15.35, p = 1.55×10^{-33}), while history-congruent choices were characterized by longer TDs ($\delta = 30.47 \pm 5.57$, T(164) = 5.47, p = 1.66×10^{-7}; Figure 3G).

Across the full spectrum of the available data, TDs showed a linear relationship with the mode of sensory processing, with shorter TDs during external mode ($\beta_1 = -4.16 \times 10^4 \pm 1.29 \times 10^3$, T($1.35 \times 10^6$) = −32.31, p = 6.03×10^{-229}, Figure 3H). However, an explorative post-hoc analysis limited to TDs that differed from the median TD by no more than 1.5 x MAD (median absolute distance[49]) indicated that, when mice engaged with the task more swiftly, TDs did indeed show a quadratic relationship with the mode of sensory processing ($\beta_2 = -1.97 \times 10^3 \pm 843.74$, T($1.19 \times 10^6$) = −2.34, p = 0.02, Figure 3I).

As in humans, it is important to ensure that ongoing changes in the sensitivity to external information are indeed driven by perceptual history and cannot be reduced to general choice biases or random behavior. Logistic regression confirmed a significant effect perceptual history on perceptual choices ($\beta = 0.51 \pm 4.49 \times 10^{-3}$, z = 112.84, p < 2.2×10^{-308}), while controlling for external sensory information ($\beta = 2.96 \pm 4.58 \times 10^{-3}$, z = 646.1, p < 2.2×10^{-308}) and general response biases toward one of the two outcomes ($\beta = -1.78 \pm 0.02$, z = −80.64, p < 2.2×10^{-308}). When eliminating perceptual history as a predictor of individual choices, AIC increased by $\delta_{AIC} = 1.48 \times 10^4$, arguing against the notion that choice randomness and general response bias are the only determinants of perceptual performance in mice (see Supplemental Figure S4C-D for parameter- and model-level inference in individual subjects).

In mice, fluctuations in the strength of history-congruent biases had a significant effect on

stimulus-congruence ($\beta_1 = -0.12 \pm 7.17 \times 10^{-4}$, $T(1.34 \times 10^6) = -168.39$, $p < 2.2 \times 10^{-308}$) beyond the effect of ongoing changes in general response biases ($\beta_2 = -0.03 \pm 6.94 \times 10^{-4}$, $T(1.34 \times 10^6) = -48.14$, $p < 2.2 \times 10^{-308}$). Eliminating the dynamic fluctuations in history-congruence as a predictor of fluctuations in stimulus-congruence resulted in an increase in AIC by $\delta_{AIC} = 2.8 \times 10^4$ (see Supplemental Section 9.2 and Supplemental Figure S5 for an in-depth assessment of general response bias).

When fitting full and history-conditioned psychometric curves to the IBL data[21], we observed that internal mode processing was associated with a history-dependent increase in bias and lapse as well as a history-independent increase in threshold (Supplemental Section 9.3.2 and Supplemental Figure S7). Over time, the frequency of history-congruent choices increased alongside stimulus-congruence and speed of response as mice were exposed to the experiment, arguing against the proposition that biases toward perceptual history reflected an unspecific response strategy in mice who were not sufficiently trained on the IBL task (Supplemental Section 9.4.2 and Supplemental Figure S8).

In sum, these analyses confirmed that the observed fluctuations in sensitivity to external sensory information are driven by dynamic changes in impact of perceptual history and cannot be reduced to general response bias and random choice behavior.

5.6 Fluctuations in mode result from coordinated changes in the impact of external and internal information on perception

The empirical data presented above indicate that, for both humans and mice, perception fluctuates between external and modes, i.e., multi-trial epochs that are characterized by enhanced sensitivity toward either external sensory information or internal predictions generated by perceptual history. Since natural environments typically show high temporal redundancy[34], previous experiences are often good predictors of new stimuli[30,31,35,41]. Serial dependencies may therefore induce autocorrelations in perception by serving as internal

predictions (or *memory* processes[9,13]) that actively integrate noisy sensory information over time[50].

Previous work has shown that such internal predictions can be built by dynamically updating the estimated probability of being in a particular perceptual state from the sequence of preceding experiences[35,46,51]. The integration of sequential inputs may lead to accumulating effects of perceptual history that progressively override incoming sensory information, enabling internal mode processing[19]. However, since such a process would lead to internal biases that may eventually become impossible to overcome[52], changes in mode may require ongoing wave-like fluctuations[9,13] in the perceptual impact of external and internal information that occur *irrespective* of the sequence of previous experiences and temporarily de-couple the decision variable from implicit internal representations of the environment[19].

Following Bayes' theorem, binary perceptual decisions depend on the log posterior ratio L of the two alternative states of the environment that participants learn about via noisy sensory information[51]. We computed the posterior by combining the sensory evidence available at time-point t (i.e., the log likelihood ratio LLR) with the prior probability ψ, weighted by the respective precision terms ω_{LLR} and ω_{ψ}:

$$L_t = LLR_t * \omega_{LLR} + \psi_t(L_{t-1}, H) * \omega_{\psi} \tag{1}$$

We derived the prior probability ψ at timepoint t from the posterior probability of perceptual outcomes at timepoint L_{t-1}. Since a switch between the two states can occur at any time, the effect of perceptual history varies according to both the sequence of preceding experiences and the estimated stability of the external environment (i.e., the *hazard rate* H[51]):

$$\psi_t(L_{t-1}, H) = L_{t-1} + log(\frac{1-H}{H} + exp(-L_{t-1})) - log(\frac{1-H}{H} + exp(L_{t-1})) \tag{2}$$

The LLR was computed from inputs s_t by applying a sigmoid function defined by parameter

α that controls the sensitivity of perception to the available sensory information (see Methods for details on s_t in humans and mice):

$$u_t = \frac{1}{1 + exp(-\alpha * s_t)} \tag{3}$$

$$LLR_t = log(\frac{u_t}{1 - u_t}) \tag{4}$$

To allow for bimodal inference, i.e., alternating periods of internally- and externally-biased modes of perceptual processing that occur irrespective of the sequence of preceding experiences, we assumed that likelihood and prior vary in their influence on the perceptual decision according to fluctuations governed by ω_{LLR} and ω_{ψ}. These anti-phase sine functions (defined by amplitudes $a_{LLR/\psi}$, frequency f and phase p) determine the precision afforded to the likelihood and prior[53]. The implicit anti-phase fluctuations are mandated by Bayes-optimal formulations in which inference depends only on the relative values of prior and likelihood precision (i.e., the Kalman gain[54]). As such, ω_{LLR} and ω_{ψ} implement a hyperprior[55] in which the likelihood and prior precisions are shifted against each other at a dominant timescale defined by f:

$$\omega_{LLR} = a_{LLR} * sin(f * t + p) + 1 \tag{5}$$

$$\omega_{\psi} = a_{\psi} * sin(f * t + p + \pi) + 1 \tag{6}$$

Finally, a sigmoid transform of the posterior L_t yields the probability of observing the perceptual decision y_t at a temperature determined by ζ^{-1}:

$$P(y_t = 1) = 1 - P(y_t = 0) = \frac{1}{1 + exp(-\zeta * L_t)} \tag{7}$$

We used a maximum likelihood procedure to fit the bimodal inference model (M1, Figure 1F) to the behavioral data from the Confidence database[20] and the IBL database[21], optimizing the parameters α, H, amp_{LLR}, amp_{ψ}, f, p and ζ (see Methods for details and Supplemental Table T2 for a summary of the parameters of the bimodal inference model). We validated our model in three steps:

First, to show that bimodal inference does not emerge spontaneously in normative Bayesian models of evidence accumulation, but requires the ad-hoc addition of anti-phase oscillations in prior and likelihood precision, we compared the bimodal inference model to four control models (M2-5, Figure 1G). In these models, we successively removed the anti-phase oscillations (M2-M4) and the integration of information across trials (M5) from the bimodal inference model and performed a model comparison based on AIC.

Model M2 ($AIC_2 = 9.76 \times 10^4$ in humans and 4.91×10^4 in mice) and Model M3 ($AIC_3 = 1.19 \times 10^5$ in humans and 5.95×10^4 in mice) incorporated only oscillations of either likelihood or prior precision. Model M4 ($AIC_4 = 1.69 \times 10^5$ in humans and 9.12×10^4 in mice) lacked any oscillations of likelihood and prior precision and corresponded to the normative model proposed by Glaze et al.[51]. In model M5 ($AIC_4 = 2.01 \times 10^5$ in humans and 1.13×10^5 in mice), we furthermore removed the integration of information across trials, such that perception depended only in incoming sensory information (Figure 1G).

The bimodal inference model achieved the lowest AIC across the full model space ($AIC_1 = 8.16 \times 10^4$ in humans and 4.24×10^4 in mice) and was clearly superior to the normative Bayesian model of evidence accumulation ($\delta_{AIC} = -8.79 \times 10^4$ in humans and -4.87×10^4 in mice; Supplemental Figure S9).

As a second validation of the bimodal inference model, we tested whether the posterior

model predicted within-training and out-of-training variables. The bimodal inference model characterizes each subject by a sensitivity parameter α (humans: $\alpha = 0.5 \pm 1.12 \times 10^{-4}$; mice: $\alpha = 1.06 \pm 2.88 \times 10^{-3}$) that captures how strongly perception is driven by the available sensory information, and a hazard rate parameter H (humans: $H = 0.45 \pm 4.8 \times 10^{-5}$; mice: $H = 0.46 \pm 2.97 \times 10^{-4}$) that controls how heavily perception is biased by perceptual history. The parameter f captures the dominant time scale at which likelihood (amplitude humans: $a_{LLR} = 0.5 \pm 2.02 \times 10^{-4}$; mice: $a_{LLR} = 0.39 \pm 1.08 \times 10^{-3}$) and prior precision (amplitude humans: $a_{\psi} = 1.44 \pm 5.27 \times 10^{-4}$; mice: $a_{\psi} = 1.71 \pm 7.15 \times 10^{-3}$) fluctuated and was estimated at $0.11 \pm 1.68 \times 10^{-5}$ $1/N_{trials}$ and $0.11 \pm 1.63 \times 10^{-4}$ $1/N_{trials}$ in mice.

As a sanity check for model fit, we tested whether the frequency of stimulus- and history-congruent trials in the Confidence database[20] and IBL database[21] correlated with the estimated parameters α and H, respectively. As expected, the estimated sensitivity toward stimulus information α was positively correlated with the frequency of stimulus-congruent perceptual choices (humans: $\beta = 8.4 \pm 0.26$, $\mathrm{T}(4.31 \times 10^3) = 32.87$, $\mathrm{p} = 1.3 \times 10^{-211}$; mice: $\beta = 1.93 \pm 0.12$, $\mathrm{T}(2.07 \times 10^3) = 16.21$, $\mathrm{p} = 9.37 \times 10^{-56}$). Likewise, H was negatively correlated with the frequency of history-congruent perceptual choices (humans: $\beta = -11.84 \pm 0.5$, $\mathrm{T}(4.29 \times 10^3) = -23.5$, $\mathrm{p} = 5.16 \times 10^{-115}$; mice: $\beta = -6.18 \pm 0.66$, $\mathrm{T}(2.08 \times 10^3) = -9.37$, $\mathrm{p} = 1.85 \times 10^{-20}$).

Our behavioral analyses reveal that humans and mice show significant effects of perceptual history that impaired performance in randomized psychophysical experiments[24,28,30,31,43] (Figure 2A and 3A). We therefore expected that humans and mice underestimated the true hazard rate $\hat{H}$ of the experimental environments (Confidence database[20]: $\hat{H}_{Humans} = 0.5 \pm 1.58 \times 10^{-5}$); IBL database[21]: $\hat{H}_{Mice} = 0.49 \pm 6.47 \times 10^{-5}$). Indeed, when fitting the bimodal inference model to the trial-wise perceptual choices, we found that the estimated (i.e., subjective) hazard rate H was lower than $\hat{H}$ for both humans ($\beta = -6.87 \pm 0.94$, $\mathrm{T}(61.87) = -7.33$, $\mathrm{p} = 5.76 \times 10^{-10}$) and mice ($\beta = -2.91 \pm 0.34$, $\mathrm{T}(112.57) = -8.51$, $\mathrm{p} = 8.65 \times 10^{-14}$).

To further probe the validity of the bimodal inference model, we asked whether posterior model quantities could explain aspects of the behavioral data that the model was not fitted to. We predicted that the posterior decision variable L_t not only encodes perceptual choices (i.e., the variable used for model estimation), but also predicts the speed of response and subjective confidence[30,44]. Indeed, the estimated trial-wise posterior decision certainty $|L_t|$ correlated negatively with RTs in humans ($\beta = -4.36 \times 10^{-3} \pm 4.64 \times 10^{-4}$, $T(1.98 \times 10^6) = -9.41$, $p = 5.19 \times 10^{-21}$) and TDs mice ($\beta = -35.45 \pm 0.86$, $T(1.28 \times 10^6) = -41.13$, $p < 2.2 \times 10^{-308}$). Likewise, subjective confidence reports were positively correlated with the estimated posterior decision certainty in humans ($\beta = 7.63 \times 10^{-3} \pm 8.32 \times 10^{-4}$, $T(2.06 \times 10^6) = 9.18$, $p = 4.48 \times 10^{-20}$).

The dynamic accumulation of information inherent to our model entails that biases toward perceptual history are stronger when the posterior decision certainty at the preceding trial is high[30,31,51]. Due to the link between posterior decision certainty and confidence, confident perceptual choices should be more likely to induce history-congruent perception at the subsequent trial[30,31]. In line with our prediction, logistic regression indicated that history-congruence was predicted by the posterior decision certainty $|L_{t-1}|$ extracted from the model (humans: $\beta = 8.22 \times 10^{-3} \pm 1.94 \times 10^{-3}$, $z = 4.25$, $p = 2.17 \times 10^{-5}$; mice: $\beta = -3.72 \times 10^{-3} \pm 1.83 \times 10^{-3}$, $z = -2.03$, $p = 0.04$) and the subjective confidence reported by the participants (humans: $\beta = 0.04 \pm 1.62 \times 10^{-3}$, $z = 27.21$, $p = 4.56 \times 10^{-163}$) at the preceding trial.

As a third validation of the bimodal inference model, we used the posterior model parameters to simulate synthetic perceptual choices and repeated the behavioral analyses conducted for the empirical data. Simulations from the bimodal inference model closely replicated our empirical results: Simulated perceptual decisions resulted from a competition of perceptual history with incoming sensory signals (Figure 4A). Stimulus- and history-congruence were significantly autocorrelated (Figure 4B-C), fluctuating in anti-phase as a scale-invariant process with a 1/f power law (Figure 4D-F). Simulated posterior certainty[28,30,44] (i.e., the

absolute of the log posterior ratio $|L_t|$) showed a quadratic relationship to the mode of sensory processing (Figure 4H), mirroring the relation of RTs and confidence reports to external and internal biases in perception (Figure 2G-H and Figure 3G-H). Crucially, the overlap between empirical and simulated data broke down when we removed the anti-phase oscillations or the accumulation of evidence over time from the bimodal inference model (Supplemental Figures S10-13).

In sum, computational modeling suggested that between-mode fluctuations are best explained by two interlinked processes (Figure 1E and F): (i), the dynamic accumulation of information across successive trials mandated by normative Bayesian models of evidence accumulation and, (ii), ongoing anti-phase oscillations in the impact of external and internal information.

6 Discussion

This work investigates the behavioral and computational characteristics of ongoing fluctuations in perceptual decision-making using two large-scale datasets in humans[20] and mice[21]. We found that humans and mice cycle through recurring intervals of reduced sensitivity to external sensory information, during which they rely more strongly on perceptual history, i.e., an internal prediction that is provided by the sequence of preceding choices. Computational modeling indicated that these slow periodicities are governed by two interlinked factors: (i), the dynamic integration of sensory inputs over time and, (ii), anti-phase oscillations in the strength at which perception is driven by internal versus external sources of information. These cross-species results suggest that ongoing fluctuations in perceptual decision-making arise not merely as a noise-related epiphenomenon of limited processing capacity, but result from a structured and adaptive mechanism that fluctuates between internally- and externally-oriented modes of sensory analysis.

6.1 Bimodal inference represents a pervasive aspect of perceptual decision-making in humans and mice

A growing body of literature has highlighted that perception is modulated by preceding choices[22–28,30,32,33]. Our work provides converging cross-species evidence supporting the notion that such serial dependencies are a pervasive and general phenomenon of perceptual decision-making (Figures 2 and 3). While introducing errors in randomized psychophysical designs[24,28,30,31,43] (Figures 2A and 3A), we found that perceptual history facilitates post-perceptual processes such as speed of response[42] (Figure 2G and 3G) and subjective confidence in humans (Figure 2I).

At the level of individual traits, increased biases toward preceding choices were associated with reduced sensitivity to external information (Supplemental Figure 1C-D) and lower metacognitive efficiency. When investigating how serial dependencies evolve over time, we observed dynamic changes in the strength of perceptual history (Figures 2 and 3B) that created wavering biases toward internally- and externally-biased modes of sensory processing. Between-mode fluctuations may thus provide a new explanation for ongoing changes in perceptual performance[6–11].

In computational terms, serial dependencies may leverage the temporal autocorrelation of natural environments[31,46] to increase the efficiency of decision-making[35,43]. Such temporal smoothing[46] of sensory inputs may be achieved by updating dynamic predictions about the world based on the sequence of noisy perceptual experiences[22,31], using algorithms based on sequential Bayes[25,42,51] such as Kalman[35] or Hierarchical Gaussian filtering[54]. At the level of neural mechanisms, the integration of internal with external information may be realized by combining feedback from higher levels in the cortical hierarchy with incoming sensory signals that are fed forward from lower levels[56].

Yet relying too strongly on serial dependencies may come at a cost: When accumulating over time, internal predictions may eventually override external information, leading to circular

and false inferences about the state of the environment[57]. Akin to the wake-sleep-algorithm in machine learning[58], bimodal inference may help to determine whether errors result from external input or from internally-stored predictions: During internal mode, sensory processing is more strongly constrained by predictive processes that auto-encode the agent's environment. Conversely, during external mode, the network is driven predominantly by sensory inputs[18]. Between-mode fluctuations may thus generate an unambiguous error signal that aligns internal predictions with the current state of the environment in iterative test-update-cycles[58]. On a broader scale, between-mode fluctuations may thus regulate the balance between feedforward versus feedback contributions to perception and thereby play a adaptive role in metacognition and reality monitoring[59].

We hypothesized that observers have certain hyperpriors that are apt for accommodating fluctuations in the predictability of their environment, i.e., people believe that their world is inherently volatile. To be Bayes optimal, it is therefore necessary to periodically re-evaluate posterior beliefs about the parameters that define an internal generative model of the external sensory environment. One way to do this is to periodically suspend the precision of prior beliefs and increase the precision afforded to sensory evidence, thus updating Bayesian beliefs about model parameters.

The empirical evidence above suggests that the timescale of this periodic scheduling of evidence accumulation may be scale-invariant. This means that there may exist a timescale of periodic fluctuations in precision over every window or length of perceptual decision-making. Bimodal inference predicts perceptual decisions under a generative model (based upon a hazard function to model serial dependencies between subsequent trials) with periodic fluctuations in the precision of sensory evidence relative to prior beliefs at a particular timescale. Remarkably, a systematic model comparison based on AIC indicated that a model with fluctuating precisions has much greater evidence, relative to a model in the absence of fluctuating precisions. This ad-hoc addition of oscillations to a normative Bayesian model of

evidence accumulation[51] allowed us to quantify the dominant timescale of periodic fluctuations mode at approximately 0.11 $1/N_{trials}$ in humans and mice that is appropriate for these kinds of paradigms.

6.2 Bimodal inference versus normative Bayesian evidence accumulation

Could bimodal inference emerge spontaneously in normative models of perceptual decision-making? In predictive processing, the relative precision of prior and likelihood determines their integration into the posterior that determines the content of perception. At the level of individual trials, the perceptual impact of internal predictions generated from perceptual history (prior precision) and external sensory information (likelihood precision) are thus necessarily anti-correlated. The same holds for mechanistic models of drift diffusion, which understand choice history biases as driven by changes in the starting point[51] or the drift rate of evidence accumulation[32]. Under the former formulation, perceptual history is bound to have a stronger influence on perception when less weight is given to incoming sensory evidence, assuming that the last choice is represented as a starting point bias. The effects of choice history in normative Bayesian and mechanistic drift diffusion models can be mapped onto one another via the Bayesian formulation of drift diffusion[60], where the inverse of likelihood precision determines the amount of noise in the accumulation of new evidence, and prior precision determines the absolute shift in its starting point[60].

While it is thus clear that the impact of perceptual history and sensory evidence are anti-correlated *at each individual trial*, we here introduce anti-phase oscillations as an ad-hoc modification to model slow fluctuations in prior and likelihood precision that evolve *over many consecutive trials* and are not mandated by normative Bayesian or mechanistic drift diffusion models. The bimodal inference model provides a reasonable explanation of the linked autocorrelations in stimulus- and history-congruence, as evidenced by formal model

comparison, successful prediction of RTs and confidence as out-of-training variables, and a qualitative reproduction of our empirical data from posterior model parameter as evidence against over- or under-fitting.

Of note, similar non-stationarities have been observed in descriptive models that assume continuous[61] or discrete[12] changes in the latent states that modulate perceptual decision-making at slow timescales. A recent computational study[62] has used a Hidden Markov model to investigate perceptual decision-making in the IBL database[21]. In analogy to our findings, the authors observed that mice switch between temporally extended *strategies* that last for more than 100 trials: During *engaged* states, perception was highly sensitive to external sensory information. During *disengaged* states, in turn, choice behavior was prone to errors due to enhanced biases toward one of the two perceptual outcomes[62]. Despite the conceptual differences to our approach (discrete states in a Hidden Markov model that correspond to switches between distinct decision-making strategies[62] vs. gradual changes in mode that emerge from sequential Bayesian inference and ongoing oscillations in the impact of external relative to internal information), it is tempting to speculate that engaged/disengaged states and between-mode fluctuations might tap into the same underlying phenomenon.

6.3 Task engagement and residual motor activation as alternative explanations for bimodal inference

As a functional explanation for bimodal inference, we propose that perception temporarily disengages from internal predictions to form stable inferences about the statistical properties of the sensory environment. Between-mode fluctuations may thus elude circular inferences that occur when both the causes and the encoding of sensory stimuli are volatile[19,57]. By the same token, we suggest that fluctuations in mode occur at the level of perceptual processing[26,30,46,47], and are not a passive phenomenon that is primarily driven by factors situated up- or downstream of sensory analysis.

How does attention relate to phenomenon of between-mode fluctuations? According to predictive processing, attention corresponds to the precision afforded to the probability distributions that underlie perceptual inference[53]. From this perspective, fluctuations between external and internal mode can be understood as ongoing shifts in the attention afforded to either external sensory information (regulated via likelihood precision) or internal predictions (regulated via prior precision). When the precision of either likelihood or prior increases, posterior precision increases, which leads to faster RTs and higher confidence. Therefore, when defined from the perspective of predictive processing as the precision afforded to likelihood and prior[53], fluctuations in attention may provide a plausible explanation for the quadratic relationship of mode to RTs and confidence (Figure 2H and J; Figure 3I, Figure 4I).

Outside of the predictive processing field, attention is often understood in the context of task engagement[63], which varies according to the availability of cognitive resources that are modulated by factors such as tonic arousal, familiarity with the task, or fatigue[63]. Our results suggest that internal mode processing cannot be completely reduced to intervals of low task engagement: In addition to shorter RTs and elevated confidence, choices during internal mode were not random or globally biased, but driven by perceptual history (Supplemental Section). Moreover, our computational model identified the dominant timescale of between-mode fluctuations at 0.11 $1/N_{trials}$, which may be compatible with fluctuations in arousal[64], but is faster than to be expected for the development of task familiarity or fatigue.

However, in interpreting the impact of between-mode fluctuations on perceptual accuracy, speed of response and confidence, it is important to consider that global modulators such as tonic arousal are known to have non-linear effects on task performance[65]: In perceptual tasks, performance seems so be highest during mid-level arousal, whereas low- and high-level arousal lead to reduced accuracy and slower responses[65]. This contrasts with the effects of bimodal inference, where accuracy increases linearly as one moves from internal to external mode, and responses become faster at both ends of the mode spectrum.

Of note, high phasic arousal has been shown to suppress biases in decision-making in humans and mice across domains[66–68], including biases toward perceptual history[28] that we implicate in internal mode processing. While the increase in response speed and history congruence over time (Supplemental Section 9.4) may argue against insufficient training as an alternative explanation for internal mode processing, it may also be indicative of waning arousal. The multiple mechanistic mappings to RTs and confidence warrant more direct measures of arousal (such as pupil size[28,65,66,68–70], motor behavior[69,70], or neural data[71]) to better delineate bimodal inference from fluctuations in global modulators of task performance.

Residual activation of the motor system may provide another contribution to serial biases in perceptual choices[72]. Such motor-driven priming may lead to errors in randomized psychophysical designs, resembling the phenomenon that we identify as internally-biased processing[73]. Moreover, residual activation of the motor system may lead to faster responses, and thus constitutes an alternative explanation for the quadratic relationship of mode with RTs[72]. The observation of elevated confidence for stronger biases toward internal mode speaks against the proposition that residual activation of the motor system is the primary driver of serial choice biases, since strong motor-driven priming should lead to frequent lapses that are typically associated reduced confidence[74]. Likewise, perceptual history effects have repeatedly been replicated in experiments with counter-balanced stimulus-response mappings[30: Feigin2021].

No-response paradigms, in which perceptual decision are inferred from eye-movements alone, could help to better differentiate perceptual from motor-related effects. Likewise, video-tracking of response behavior and neural recording from motor- and premotor, which has recently been released for the IBL database[IBL2023], may provide further insight into the relation of motor behavior to the perceptual phenomenon of between-mode fluctuations.

6.4 Limitations and open questions

Our results suggest bimodal inference as a pervasive aspect of perceptual decision-making in humans and mice. However, a number of limitations and open questions have to be considered:

First, this work sought to understand whether fluctuations between internal and external mode, which we initially observed in an experiment on bistable perception in humans[19], represent a general phenomenon that occurs across a diverse set of perceptual decision-making tasks. Our analysis of the Confidence database[20] therefore collapsed across all available experiments on binary perceptual decision-making. Individual experiments differed with respect to the stimuli, the manipulation of difficulty, the timing of trials, and the way responses were collected, but were highly comparable with respect to the central variables of stimulus- and history-congruence (Supplemental Figure S1A-B).

The variability across experiments, which we considered as random effects in all statistical analyses, enabled us to assess whether bimodal inference represents a general phenomenon in perceptual decision-making, but limited the precision at which we were able to investigate the relation of mode to behavioral variables such as timing, task difficulty, RT or confidence. This issue is partially resolved by our analyses of the IBL database, which replicated our findings in an experiment that was highly standardized with respect to timing, task difficulty, and behavioral read-out[21]. It will be an important task for future research to validate our results on bimodal inference in a standardized dataset of comparable volume in humans, which is, to our knowledge, not yet available.

Second, our results point to an attraction of perception toward preceding choices. Previous work has shown that perceptual decision-making is concurrently affected by both attractive and repulsive serial biases that operate on distinct time-scales and serve complementary functions for sensory processing[27,75,76]: Short-term attraction may serve the decoding of noisy sensory inputs and increase the stability of perception, whereas long-term repulsion may

enable efficient encoding and sensitivity to change[27]. In the data analyzed here, history biases tended to be repetitive (Figure 2A, Figure 3A, Supplemental Figure S6 and S7), and only 2 of the 66 experiments of the Confidence database[20] showed significant alternating biases (Supplemental Figure S1). However, as we show in Supplemental Figure S14, fluctuations in both alternating and repeating history biases generate overlapping autocorrelation curves. Our analysis of between-mode fluctuations is therefore not tied exclusively to repeating biases, but accommodates alternating biases as well, such that both may lead to internally-biased processing and reduced sensitivity to external sensory information. Future work could apply our approach to paradigms that boost alternating as opposed to repeating biases, as this would help to better understand how repetition and alternation are linked in terms of their computational function and neural implementation[27].

A third open question concerns the computational underpinnings of bimodal inference. The addition of slow anti-phase oscillations to the integration of prior and likelihood represents an ad-hoc modification of a normative Bayesian model of evidence accumulation[51]. While the bimodal inference model is supported by formal model comparison, the successful prediction of out-of-training variables and the qualitative reproduction of our empirical data in simulations from posterior model parameters, it is an important task for future research to test (i), whether between-mode fluctuations can emerge spontaneously in hierarchical models of Bayesian inference, (ii), whether modes are continuous[19] or discrete[62], and (iii), whether bimodal inference can be causally manipulated by experimental variables. We speculate that between-mode fluctuations may separate the perceptual contribution of internal predictions and external sensory data in time, creating unambiguous learning signals that benefit inference about the precision of prior and likelihood, respectively. This proposition should be tested empirically by relating the phenomenon of bimodal inference to performance in, e.g., reversal learning, probabilistic reasoning, or metacognition.

A final important avenue for further research on bimodal inference is to elucidate its neurobi-

ological underpinnings. Since between-mode fluctuations were found in humans and mice, future studies can apply non-invasive and invasive neuro-imaging and electrophysiology to better understand the neural mechanisms that generate ongoing changes in mode in terms of their neuro-anatomy, -chemistry and -circuitry.

Establishing the neural correlates of externally- an internally-biased modes will enable exiting opportunities to investigate their role for adaptive perception and decision-making: Causal interventions via pharmacological challenges, optogenetic manipulations or (non-)invasive brain stimulation will help to understand whether between-mode fluctuations are implicated in resolving credit-assignment problems[18,77] or in calibrating metacognition and reality monitoring[59]. Answers to these questions may provide new insights into the pathophysiology of hallucinations and delusions, which have been characterized by an imbalance in the impact of external versus internal information[56,78,79] and are typically associated with metacognitive failures and a departure from consensual reality[79].

7 Methods

7.1 Resource availability

7.1.1 Lead contact

Further information and requests for resources should be directed to and will be fulfilled by the lead contact, Veith Weilnhammer (veith.weilnhammer@gmail.com).

7.1.2 Materials availability

This study did not generate new unique reagents.

7.1.3 Data and code availability

All custom code and behavioral data are available on https://github.com/veithweilnhammer/Modes. This manuscript was created using the *R Markdown* framework, which integrates all data-related computations and the formatted text within one document. With this, we wish to make our approach fully transparent and reproducible for reviewers and future readers.

7.2 Experimental model and subject details

7.2.1 Confidence database

We downloaded the human data from the Confidence database[20] on 10/21/2020, limiting our analyses to the category *perception*. Within this category, we selected studies in which participants made binary perceptual decisions between two alternatives. We excluded two experiments in which the average perceptual accuracy fell below 50%. After excluding these experiments, our sample consisted of 21.05 million trials obtained from 4317 human participants and 66 individual experiments (Supplemental Table 1). Out of the 66 included experiments, 62 investigated visual, 1 auditory, 2 proprioceptive, and 1 multimodal perception. 59 experiments were based on discrimination and 6 on detection, with one investigating both.

7.2.2 IBL database

We downloaded the data from the IBL database[21] on 04/28/2021. We limited our analyses to the *basic task*, during which mice responded to gratings that appeared with equal probability in the left or right hemifield. Within each mouse, we excluded sessions in which perceptual accuracy was below 80% for stimuli presented at a contrast $\geq 50\%$. After exclusion, our sample consisted of 1.46 million trials trials obtained from N = 165 mice.

7.3 Method details

7.3.1 Variables of interest

Primary variables of interest: We extracted trial-wise data on the presented stimulus and the associated perceptual decision. Stimulus-congruent choices were defined by perceptual decisions that matched the presented stimuli. History-congruent choices were defined by perceptual choices that matched the perceptual choice at the immediately preceding trial. The dynamic probabilities of stimulus- and history-congruence were computed in sliding windows of ± 5 trials.

The *mode* of sensory processing was derived by subtracting the dynamic probability of history-congruence from the dynamic probability of stimulus-congruence, such that positive values indicate externally-oriented processing, whereas negative values indicate internally-oriented processing. When visualizing the relation of the mode of sensory processing to confidence, RTs or trial duration (see below), we binned the mode variable in 10% intervals. We excluded bins that contained less than 0.5% of the total number of available data-points.

Secondary variables of interest: From the Confidence Database[20], we furthermore extracted trial-wise confidence reports and RTs. Out of the 58 experiments that provide information on RTs, 46 cued the response by the onset of a response screen or an additional response cue, whereas 14 allowed participants to response at any time after stimulus onset. If RTs were available for both the perceptual decision and the confidence report, we only

extracted the RT associated with the perceptual decision. To enable comparability between studies, we normalized RTs and confidence reports within individual studies using the *scale* R function. If not available for a particular study, RTs were treated as missing variables. From the IBL database[21], we extracted trial durations (TDs) as defined by interval between stimulus onset and feedback, which represents a coarse measure of RT[21].

Exclusion criteria for individual data-points: For non-normalized data (TDs from the IBL database[21]; d-prime, meta-dprime and M-ratio from the Confidence database[20] and simulated confidence reports), we excluded data-points that differed from the median by more than 3 x MAD (median absolute distance[49]). For normalized data (RTs and confidence reports from the Confidence database[20]), we excluded data-points that differed from the mean by more than 3 x SD (standard deviation).

7.3.2 Control variables

Next to the sequence of presented stimuli, we assessed the autocorrelation of task difficulty as an alternative explanation for any autocorrelation in stimulus- and history-congruence. In the Confidence Database[20], 21 of the 66 included experiments used fixed difficulty levels, whereas 45 manipulated difficulty levels within participants. Difficulty was manipulated via noise masks, contrast, luminance, presentation time, or stimulus probability for gabors, dot coherence for random dot kinematograms, difference in elements and set size for comparisons of numerosity, difference in clicks for auditory discrimination, temporal distance for meta-contrast masking, and amount of self-motion for proprioception. We treated task difficulty as a missing variable for the experiments that fixed it at the participant-level, as this precluded the computation of autocorrelation curves. In analogy to RTs and confidence, difficulty levels were normalized within individual studies. For the IBL Database[21], task difficulty was defined by the contrast of the presented grating.

7.3.3 Autocorrelations

For each participant, trial-wise autocorrelation coefficients were estimated using the R-function *acf* with a maximum lag defined by the number of trials available per subject. Autocorrelation coefficients are displayed against the lag (in numbers of trials, ranging from 1 to 20) relative to the index trial (t = 0; Figure 2B-C, 3B-C and 4B-C). To account for spurious autocorrelations that occur due to imbalances in the analyzed variables, we estimated autocorrelations for randomly permuted data (100 iterations). For group-level autocorrelations, we computed the differences between the true autocorrelation coefficients and the mean autocorrelation observed for randomly permuted data and averaged across participants.

At a given trial, group-level autocorrelation coefficients were considered significant when linear mixed effects modeling indicated that the difference between real and permuted autocorrelation coefficients was above zero at an alpha level of 0.05%. To test whether the autocorrelation of stimulus- and history-congruence remained significant when controlling for task difficulty and the sequence of presented stimuli, we added the respective autocorrelation as an additional factor to the linear mixed effects model that computed the group-level statistics (see also *Mixed effects modeling*).

To assess autocorrelations at the level of individual participants, we counted the number of subsequent trials (starting at the first trial after the index trial) for which less than 50% of the permuted autocorrelation coefficients exceeded the true autocorrelation coefficient. For example, a count of zero indicates that the true autocorrelation coefficients exceeded *less than 50%* of the autocorrelation coefficients computed for randomly permuted data at the first trial following the index trial. A count of five indicates that, for the first five trials following the index trial, the true autocorrelation coefficients exceeded *more than 50%* of the respective autocorrelation coefficients for the randomly permuted data; at the 6th trial following the index trial, however, *less than 50%* of the autocorrelation coefficients exceeded the respective permuted autocorrelation coefficients.

7.3.4 Spectral analysis

We used the R function *spectrum* to compute the spectral densities for the dynamic probabilities of stimulus- and history-congruence as well as the phase (i.e., frequency-specific shift between the two time-series ranging from 0 to $2 * \pi$) and squared coherence (frequency-specific variable that denotes the degree to which the shift between the two time-series in constant, ranging from 0 to 100%). Periodograms were smoothed using modified Daniell smoothers at a width of 50.

Since the dynamic probabilities of history- and stimulus-congruence were computed using a sliding windows of ± 5 trials (i.e., intervals containing a total of 11 trials), we report the spectral density, coherence and phase for frequencies below 1/11 $1/N_{trials}$. Spectral densities have one value per subject and frequency (data shown in Figures 2D and 3D). To assess the relation between stimulus- and history-congruence in this frequency range, we report average phase and average squared coherence for all frequencies below 1/11 $1/N_{trials}$ (i.e., one value per subject; data shown in Figure 2E-F and 3E-F).

Since the data extracted from the Confidence Database[20] consist of a large set of individual studies that differ with respect to inter-trial intervals, we defined the variable *frequency* in the dimension of cycles per trial $1/N_{trials}$ rather than cycles per second (Hz). For consistency, we chose $1/N_{trials}$ as the unit of frequency for the IBL database[21] as well.

7.4 Quantification and statistical procedures

All aggregate data are reported and displayed with errorbars as mean $\pm$ standard error of the mean.

7.4.1 Mixed effects modeling

Unless indicated otherwise, we performed group-level inference using the R-packages *lmer* and *afex* for linear mixed effects modeling and *glmer* with a binomial link-function for logistic

regression. We compared models based on AIC. To account for variability between the studies available from the Confidence Database[20], mixed modeling was conducted using random intercepts defined for each study. To account for variability across experimental session within the IBL database[21], mixed modeling was conducted using random intercepts defined for each individual session. When multiple within-participant datapoints were analyzed, we estimated random intercepts for each participant that were *nested* within the respective study of the Confidence database[20]. By analogy, for the IBL database[21], we estimated random intercepts for each session that were nested within the respective mouse. We report β values referring to the estimates provided by mixed effects modeling, followed by the respective T statistic (linear models) or z statistic (logistic models).

The effects of stimulus- and history-congruence on RTs and confidence reports (Figure 2, 3 and 4, subpanels G-I) were assessed in linear mixed effects models that tested for main effects of both stimulus- and history-congruence as well as the between-factor interaction. Thus, the significance of any effect of history-congruence on RTs and confidence reports was assessed while controlling for the respective effect of stimulus-congruence (and vice versa).

7.4.2 Psychometric function

We obtained psychometric curves by fitting the following error function to the behavioral data:

$$y_p = \gamma + (1 - \gamma - \delta) * (erf(\frac{s_w + \mu}{t}) + 1)/2 \tag{8}$$

We used the Broyden–Fletcher–Goldfarb–Shanno algorithm in maximum likelihood estimation[80] to predict individual choices y (outcome A: $y = 0$; outcome B: $y = 1$) from the choice probability y_p. In humans, we computed s_w by multiplying the inputs s (stimulus A: 0; outcome B: 1) with the task difficulty D_b (binarized across 7 levels):

$$s_w = (s - 0.5) * D_b \tag{9}$$

In mice, s_w was defined by the respective stimulus contrast in the two hemifields:

$$s_w = Contrast_{Right} - Contrast_{Left} \tag{10}$$

Parameters of the psychometric error function were fitted using the R-package *optimx*[80]. The psychometric error function was defined via the parameters γ (lower lapse; lower bound = 0, upper bound = 0.5), δ (upper lapse; lower bound = 0, upper bound = 0.5), μ (bias; lower bound humans = -5; upper bound humans = 5, lower bound mice = -0.5, upper bound mice = 0.5) and threshold t (lower bound humans = 0.5, upper bound humans = 25; lower bound mice = 0.01, upper bound mice = 1.5).

7.4.3 Computational modeling

Model definition: Our modeling analysis is an extension of a model proposed by Glaze et al.[51], who defined a normative account of evidence accumulation for decision-making. In this model, trial-wise choices are explained by applying Bayes theorem to infer moment-by-moment changes in the state of environment from trial-wise noisy observations across trials.

Following Glaze et al.[51], we applied Bayes rule to compute the posterior evidence for the two alternative choices (i.e., the log posterior ratio L) from the sensory evidence available at time-point t (i.e., the log likelihood ratio LLR) with the prior probability ψ, weighted by the respective precision terms ω_{LLR} and ω_{ψ}:

$$L_t = LLR_t * \omega_{LLR} + \psi_t(L_{t-1}, H) * \omega_{\psi} \tag{11}$$

In the trial-wise design studied here, a transition between the two states of the environment

(i.e., the sources generating the noisy observations available to the participant) can occur at any time. Despite the random nature of the psychophysical paradigms studied here[20,21], humans and mice showed significant biases toward preceding choices (Figure 2A and 3A). We thus assumed that the prior probability of the two possible outcomes depends on the posterior choice probability at the preceding trial and the hazard rate H assumed by the participant. Following Glaze et al.[51], the prior ψ is thus computed as follows:

$$\psi_t(L_{t-1}, H) = L_{t-1} + log(\frac{1-H}{H} + exp(-L_{t-1})) - log(\frac{1-H}{H} + exp(L_{t-1})) \tag{12}$$

In this model, humans, mice and simulated agents make perceptual choices based on noisy observations u. The are computed by applying a sensitivity parameter α to the content of external sensory information s. For humans, we defined the input s by the two alternative states of the environment (stimulus A: $s = 0$; stimulus B: $s = 1$), which generated the observations u through a sigmoid function that applied a sensitivity parameter α:

$$u_t = \frac{1}{1 + exp(-\alpha * (s_t - 0.5))} \tag{13}$$

In mice, the inputs s were defined by the respective stimulus contrast in the two hemifields:

$$s_t = Contrast_{Right} - Contrast_{Left} \tag{14}$$

As in humans, we derived the input u by applying a sigmoid function with a sensitivity parameter α to input s:

$$u_t = \frac{1}{1 + exp(-\alpha * s_t)} \tag{15}$$

For humans, mice and in simulations, the log likelihood ratio LLR was computed from u as

follows:

$$LLR_t = log(\frac{u_t}{1-u_t}) \tag{16}$$

To allow for long-range autocorrelation in stimulus- and history-congruence (Figure 2B and 3B), our modeling approach differed from Glaze et al.[51] in that it allowed for systematic fluctuation in the impact of sensory information (i.e., LLR) and the prior probability of choices ψ on the posterior probability L. This was achieved by multiplying the log likelihood ratio and the log prior ratio with coherent anti-phase fluctuations according to $\omega_{LLR} = a_{LLR} * sin(f * t + phase) + 1$ and $\omega_{\psi} = a_{\psi} * sin(f * t + phase + \pi) + 1$.

Model fitting: In model fitting, we predicted the trial-wise choices y_t (option A: 0; option B: 1) from inputs s. To this end, we minimized the log loss between y_t and the choice probability y_{pt} in the unit interval. y_{pt} was derived from L_t using a sigmoid function defined by the inverse decision temperature ζ:

$$y_{pt} = \frac{1}{1 + exp(-\zeta * L_t)} \tag{17}$$

This allowed us to infer the free parameters H (lower bound = 0, upper bound = 1; human posterior = $0.45 \pm 4.8 \times 10^{-5}$; mouse posterior = $0.46 \pm 2.97 \times 10^{-4}$), α (lower bound = 0, upper bound = 5; human posterior = $0.5 \pm 1.12 \times 10^{-4}$; mouse posterior = $1.06 \pm 2.88 \times 10^{-3}$), a_{ψ} (lower bound = 0, upper bound = 10; human posterior = $1.44 \pm 5.27 \times 10^{-4}$; mouse posterior = $1.71 \pm 7.15 \times 10^{-3}$), amp_{LLR} (lower bound = 0, upper bound = 10; human posterior = $0.5 \pm 2.02 \times 10^{-4}$; mouse posterior = $0.39 \pm 1.08 \times 10^{-3}$), frequency f (lower bound = 1/40, upper bound = 1/5; human posterior = $0.11 \pm 1.68 \times 10^{-5}$; mouse posterior = $0.11 \pm 1.63 \times 10^{-4}$), p (lower bound = 0, upper bound = $2 * \pi$; human posterior = $2.72ś4.41 \times 10^{-4}$; mouse posterior = $2.83 \pm 3.95 \times 10^{-3}$) and inverse decision temperature ζ (lower bound = 1, upper bound = 10; human posterior = $4.63 \pm 1.95 \times 10^{-4}$; mouse posterior

$= 4.82 \pm 3.03 \times 10^{-3}$) using maximum likelihood estimation with the Broyden–Fletcher–Goldfarb–Shanno algorithm as implemented in the R-function *optimx*[80] (see Supplemental Table T2 for a description of our model parameters).

We validated the bimodal inference model in three steps: a formal model comparison to reduced models based on AIC (Figure 1F-G; Supplemental Figure S9), the prediction of within-training (stimulus- and history-congruence) as well as out-of-training variables (RT and confidence), and a qualitative reproduction of the empirical data from model simulations based on estimated parameters (Figure 4).

Model comparison. We assessed the following model space based on AIC:

- The full *bimodal inference model* (M1; Figure 1F) incorporates the influence of sensory information according to the parameter α (likelihood); the integration of evidence across trials according to the parameter H (prior); anti-phase oscillations in between likelihood and prior precision according to ω_{LLR} and ω_{ψ} with parameters a_{LLR} (amplitude likelihood fluctuation), a_{ψ} (amplitude prior fluctuation), f (frequency) and p (phase).

- The *likelihood-oscillation-only model* (M2; Figure 1G) incorporates the influence of sensory information according to parameter α (likelihood); the integration of evidence across trials according to parameter H (prior); oscillations in likelihood precision according to ω_{LLR} with parameters a_{LLR} (amplitude likelihood fluctuation), f (frequency) and p (phase).

- The *prior-oscillation-only model* (M3; Figure 1G) incorporates the influence of sensory information according to parameter α (likelihood); the integration of evidence across trials according to parameter H (prior); oscillations in the prior precision according to ω_{ψ} with parameters a_{ψ} (amplitude prior fluctuation), f (frequency) and p (phase). Please note that all models M1-3 lead to shifts in the relative precision of likelihood and prior.

- The *normative-evidence-accumulation* (M4; Figure 1G) incorporates the influence of sensory information according to parameter α (likelihood); the integration of evidence across trials according to parameter H (prior), There are no additional oscillations. Model M4 thus corresponds to the model proposed by Glaze et al. and captures normative evidence accumulation in unpredictable environments using a Bayesian update scheme[51]. The comparison against M4 tests the null hypothesis that fluctuations in mode emerge from a normative Bayesian model without the ad-hoc addition of oscillations as in models M1-3.

- The *no-evidence-accumulation* (M5; Figure 1G) incorporates the influence of sensory information according to parameter α (likelihood). The model lacks integration of evidence across trials (flat prior) and oscillations. The comparison against M5 tests the null hypothesis that observers do not use prior information derived from serial dependency in perception.

Prediction of within-training and out-of-training variables. To validate our model, we correlated individual posterior parameter estimates with the respective conventional variables. As a sanity check, we tested (i), whether the estimated hazard rate H correlated negatively with the frequency of history-congruent choices and, (ii), whether the estimated sensitivity to sensory information α correlated positively with the frequency of stimulus-congruent choices. In addition, we tested whether the posterior decision certainty (i.e.. the absolute of the log posterior ratio) correlated negatively with RTs and positively with confidence. This allowed us to assess whether our model could explain aspects of the data it was not fitted to (i.e., RTs and confidence).

Simulations. Finally, we used simulations (Figure 4, Supplemental Figures S10-13) to show that all model components, including the anti-phase oscillations governed by a_ψ, a_{LLR}, f and p, were necessary for our model to reproduce the characteristics of the empirical data. This enabled us to assess over- or under-fitting in the bimodal inference model and

all reduced models M2-M5. We used the posterior model parameters observed for humans (H, α, a_ψ, a_{LLR}, f, p and ζ) to define individual parameters for simulation in 4317 simulated participants (i.e., equivalent to the number of human participants). For each participant, the number of simulated trials was drawn at random between 300 to 700. Inputs s were drawn at random for each trial, such that the sequence of inputs to the simulation did not contain any systematic seriality. Noisy observations u were generated by applying the posterior parameter α to inputs s, thus generating stimulus-congruent choices in $71.36 \pm 2.6 \times 10^{-3}\%$ of trials. Choices were simulated based on the trial-wise choice probabilities y_p obtained from our model. Simulated data were analyzed in analogy to the human and mouse data. As a substitute of subjective confidence, we computed the absolute of the trial-wise log posterior ratio $|L|$ (i.e., the posterior decision certainty).

8 Figures

8.1 Figure 1

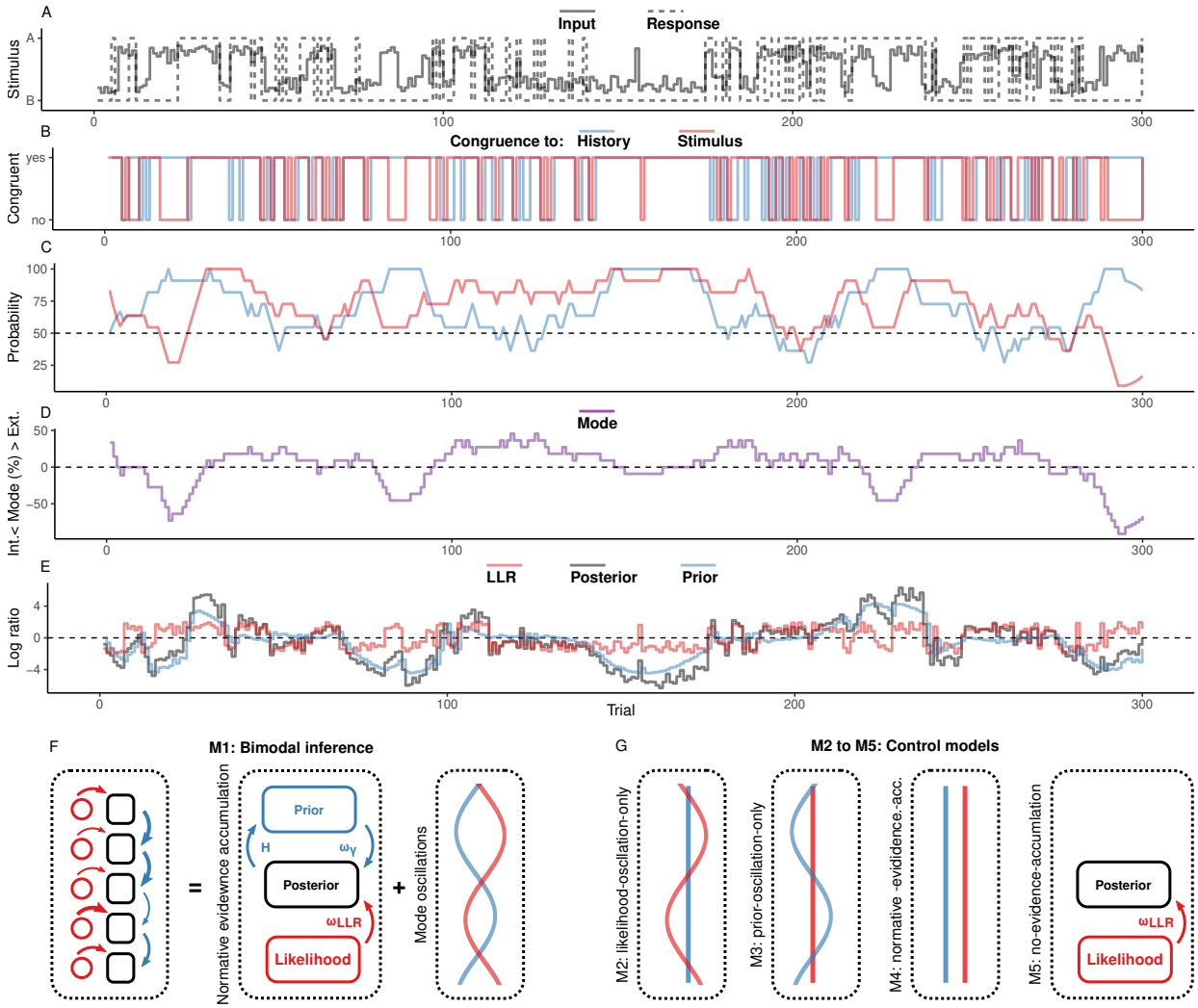

Figure 1. Concept.

A. In binary perceptual decision-making, a participant is presented with stimuli from two categories (A vs. B; dotted line) and reports consecutive perceptual choices via button presses (sold line). All panels below refer to these stimulated example data.

B. When the response matches the external stimulus information (i.e., overlap between dotted and solid line in panel A), perceptual choices are *stimulus-congruent* (red line). When the response matches the response at the preceding trial, perceptual choices are *history-congruent*

(blue line).

C. The dynamic probabilities of stimulus- and history-congruence (i.e., computed in sliding windows of ±5 trials) fluctuate over time.

D. The *mode* of perceptual processing is derived by computing the difference between the dynamic probabilities of stimulus- and history-congruence. Values above 0% indicate a bias toward external information, whereas values below 0% indicate a bias toward internal information.

E. In computational modeling, internal mode is caused by an enhanced impact of perceptual history. This causes the posterior (black line) to be close to the prior (blue line). Conversely, during external mode, the posterior is close to the sensory information (log likelihood ratio, red line).

F. The bimodal inference model (M1) explains fluctuations between externally- and externally-biased modes (left panel) by two interacting factors: a normative accumulation of evidence according to parameters H (middle panel), and anti-phase oscillations in the precision terms ω_{LLR} and ω_{ψ} (right panel).

G. The control models M2-M5 were constructed by successively removing the anti-phase oscillations and the integration of information from the bimodal inference model. Please note that the normative-evidence-accumulation-model (M4) corresponds to the model proposed by Glaze et al.[51]. In the no-evidence-accumulation model (M5), perceptual decisions depend only on likelihood information (flat priors).

8.2 Figure 2

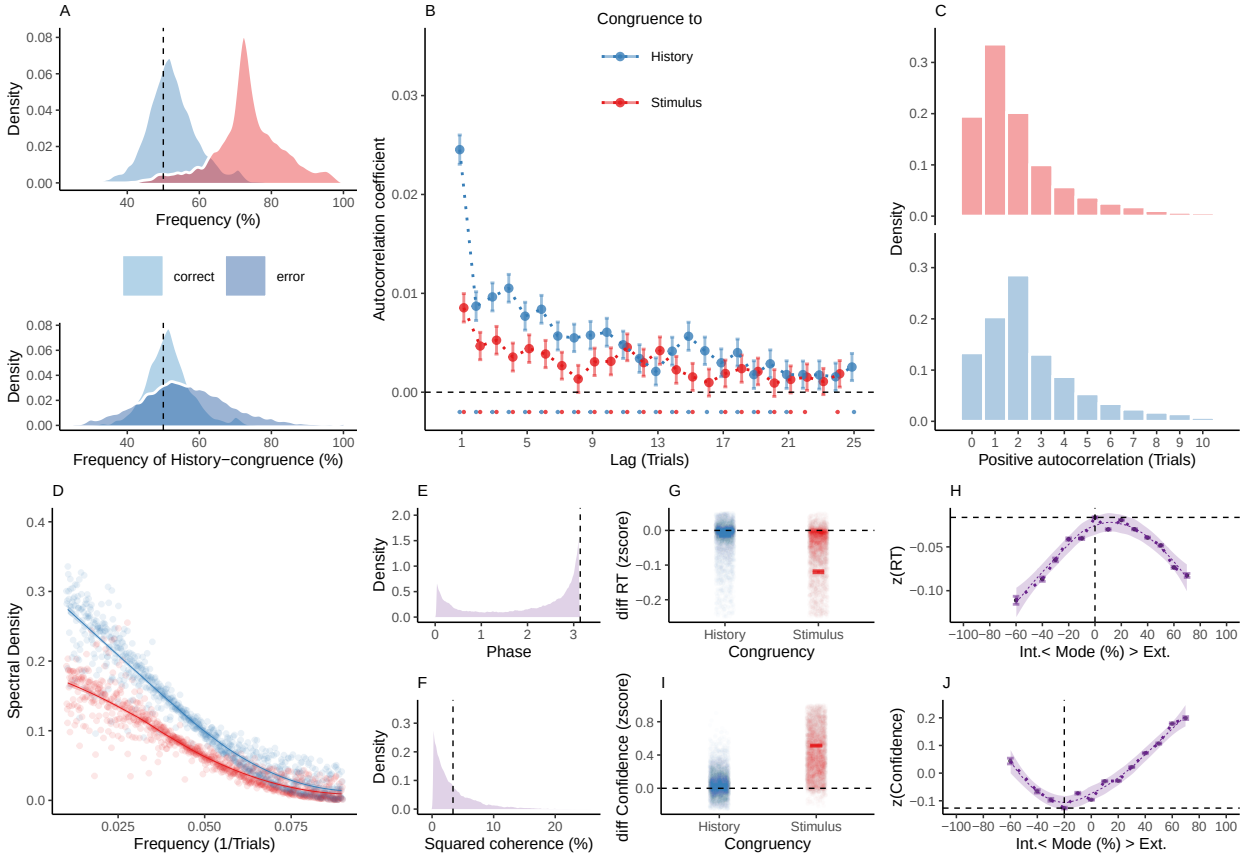

Figure 2. Internal and external modes in human perceptual decision-making.

A. In humans, perception was stimulus-congruent in 73.46% ± 0.15% (in red) and history-congruent in 52.7% ± 0.12% of trials (in blue; upper panel). History-congruent perceptual choices were more frequent when perception was stimulus-incongruent (i.e., on *error* trials; lower panel), indicating that history effects impair performance in randomized psychophysical designs.

B. Relative to randomly permuted data, we found highly significant autocorrelations of stimulus-congruence and history-congruence (dots indicate intercepts $\neq 0$ in trial-wise linear mixed effects modeling at $p < 0.05$). Across trials, the autocorrelation coefficients were best fit by an exponential function (adjusted R^2 for stimulus-congruence: 0.53; history-congruence: 0.72) as compared to a linear function (adjusted R^2 for stimulus-congruence: 0.53; history-congruence: 0.51), decaying at a rate of $\gamma = -1.92 \times 10^{-3} \pm 4.5 \times 10^{-4}$ ($T(6.88 \times 10^4)$

$= -4.27$, $p = 1.98 \times 10^{-5}$) for stimulus-congruence and at a rate of $\gamma = -6.11 \times 10^{-3} \pm 5.69 \times 10^{-4}$ ($T(6.75 \times 10^4) = -10.74$, $p = 7.18 \times 10^{-27}$) for history-congruence.

C. Here, we depict the number of consecutive trials at which autocorrelation coefficients exceeded the respective autocorrelation of randomly permuted data within individual participants. For stimulus-congruence (upper panel), the lag of positive autocorrelation amounted to $3.24 \pm 2.39 \times 10^{-3}$ on average, showing a peak at trial t+1 after the index trial. For history-congruence (lower panel), the lag of positive autocorrelation amounted to $4.87 \pm 3.36 \times 10^{-3}$ on average, peaking at trial t+2 after the index trial.

D. The smoothed probabilities of stimulus- and history-congruence (sliding windows of ± 5 trials) fluctuated as a scale-invariant process with a 1/f power law, i.e., at power densities that were inversely proportional to the frequency.

E. The distribution of phase shift between fluctuations in stimulus- and history-congruence peaked at half a cycle (π denoted by dotted line).

F. The average squared coherence between fluctuations in stimulus- and history-congruence (black dotted line) amounted to $6.49 \pm 2.07 \times 10^{-3}\%$

G. We observed faster RTs for both stimulus-congruence (as opposed to stimulus-incongruence, $\beta = -0.14 \pm 1.6 \times 10^{-3}$, $T(1.99 \times 10^6) = -85.84$, $p < 2.2 \times 10^{-308}$) and history-congruence ($\beta = -9.56 \times 10^{-3} \pm 1.37 \times 10^{-3}$, $T(1.98 \times 10^6) = -6.97$, $p = 3.15 \times 10^{-12}$).

H. The mode of perceptual processing (i.e., the difference between the smoothed probability of stimulus- vs. history-congruence) showed a quadratic relationship to RTs, with faster RTs for stronger biases toward both external sensory information and internal predictions provided by perceptual history ($\beta_2 = -19.86 \pm 0.52$, $T(1.98 \times 10^6) = -38.43$, $p = 5 \times 10^{-323}$). The horizontal and vertical dotted lines indicate maximum RT and the associated mode, respectively.

I. Confidence was enhanced for both stimulus-congruence (as opposed to stimulus-

incongruence, $\beta = 0.48 \pm 1.38 \times 10^{-3}$, $T(2.06 \times 10^6) = 351.54$, $p < 2.2 \times 10^{-308}$) and history-congruence ($\beta = 0.04 \pm 1.18 \times 10^{-3}$, $T(2.06 \times 10^6) = 36.85$, $p = 3.25 \times 10^{-297}$).

J. In analogy to RTs, we found a quadratic relationship between the mode of perceptual processing and confidence, which increased when both externally- and internally-biased modes grew stronger ($\beta_2 = 39.3 \pm 0.94$, $T(2.06 \times 10^6) = 41.95$, $p < 2.2 \times 10^{-308}$). The horizontal and vertical dotted lines indicate minimum confidence and the associated mode, respectively.

8.3 Figure 3

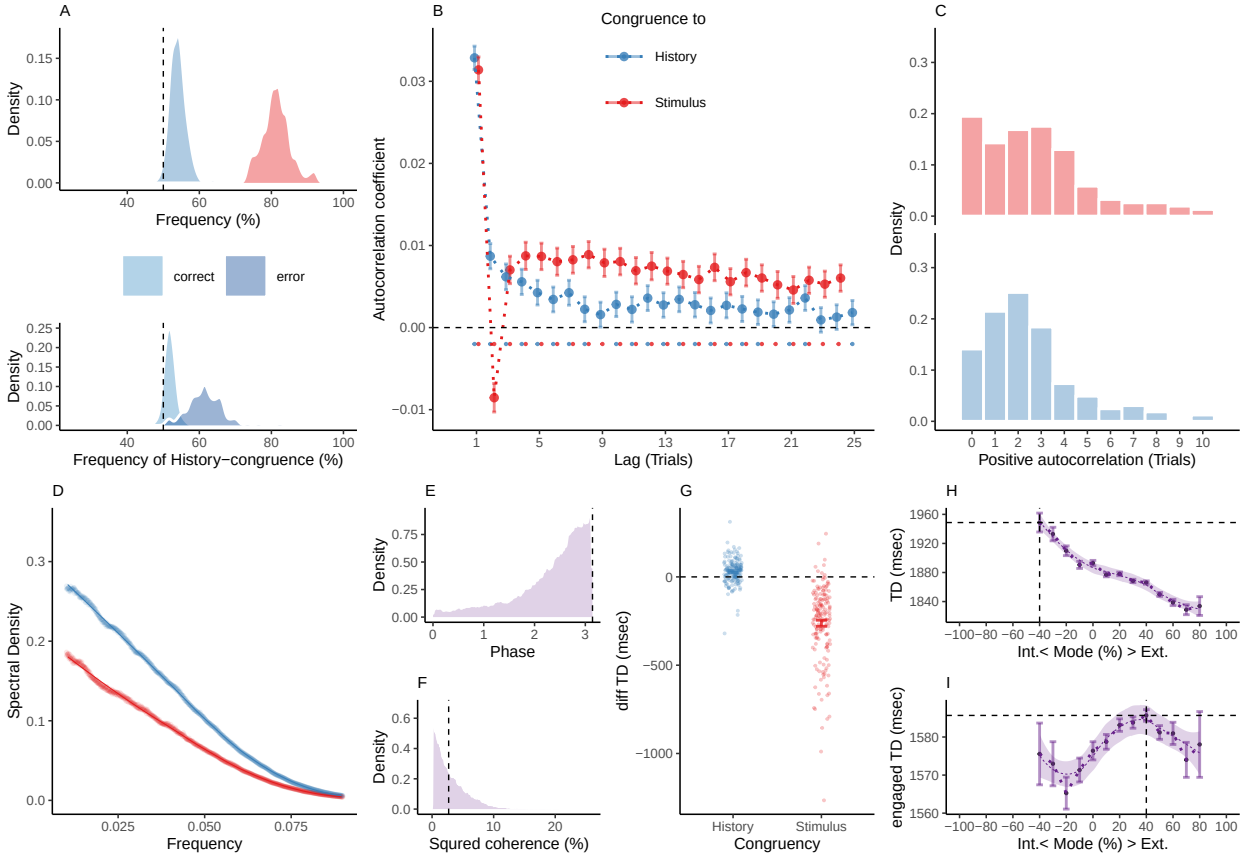

Figure 3. Internal and external modes in mouse perceptual decision-making.

A. In mice, 81.37% ± 0.3% of trials were stimulus-congruent (in red) and 54.03% ± 0.17% of trials were history-congruent (in blue; upper panel). History-congruent perceptual choices were not a consequence of the experimental design, but a source of error, as they were more frequent on stimulus-incongruent trials (lower panel).

B. Relative to randomly permuted data, we found highly significant autocorrelations of stimulus-congruence and history-congruence (dots indicate intercepts $\neq 0$ in trial-wise linear mixed effects modeling at $p < 0.05$). Please note that the negative autocorrelation of stimulus-congruence at trial 2 was a consequence of the experimental design (Supplemental Figure 2D-F). As in humans, autocorrelation coefficients were best fit by an exponential function (adjusted R^2 for stimulus-congruence: 0.44; history-congruence: 0.52) as compared to a linear function (adjusted R^2 for stimulus-congruence: 3.16×10^{-3}; history-congruence:

0.26), decaying at a rate of $\gamma = -6.2 \times 10^{-4} \pm 5.93 \times 10^{-4}$ ($T(3.55 \times 10^4) = -1.05$, $p = 0.3$) for stimulus-congruence and at a rate of $\gamma = -6.7 \times 10^{-3} \pm 5.94 \times 10^{-4}$ ($T(3.69 \times 10^4) = -11.27$, $p = 2.07 \times 10^{-29}$) for history-congruence.

C. For stimulus-congruence (upper panel), the lag of positive autocorrelation was longer in comparison to humans (4.59 ± 0.06 on average). For history-congruence (lower panel), the lag of positive autocorrelation was slightly shorter relative to humans (2.58 ± 0.01 on average, peaking at trial t+2 after the index trial).

D. In mice, the dynamic probabilities of stimulus- and history-congruence (sliding windows of ± 5 trials) fluctuated as a scale-invariant process with a 1/f power law.

E. The distribution of phase shift between fluctuations in stimulus- and history-congruence peaked at half a cycle (π denoted by dotted line).

F. The average squared coherence between fluctuations in stimulus- and history-congruence (black dotted line) amounted to $3.45 \pm 0.01\%$.

G. We observed shorter trial durations (TDs) for stimulus-congruence (as opposed to stimulus-incongruence, $\beta = -1.12 \pm 8.53 \times 10^{-3}$, $T(1.34 \times 10^6) = -131.78$, $p < 2.2 \times 10^{-308}$), but longer TDs for history-congruence ($\beta = 0.06 \pm 6.76 \times 10^{-3}$, $T(1.34 \times 10^6) = 8.52$, $p = 1.58 \times 10^{-17}$).

H. TDs decreased monotonically for stronger biases toward external mode ($\beta_1 = -4.16 \times 10^4 \pm 1.29 \times 10^3$, $T(1.35 \times 10^6) = -32.31$, $p = 6.03 \times 10^{-229}$). The horizontal and vertical dotted lines indicate maximum TD and the associated mode, respectively.

I. For TDs that differed from the median TD by no more than 1.5 x MAD (median absolute distance[49]), mice exhibited a quadratic component in the relationship between the mode of sensory processing and TDs ($\beta_2 = -1.97 \times 10^3 \pm 843.74$, $T(1.19 \times 10^6) = -2.34$, $p = 0.02$). This explorative post-hoc analysis focuses on trials at which mice engage more swiftly with the experimental task. The horizontal and vertical dotted lines indicate maximum TD and

the associated mode, respectively.

8.4 Figure 4

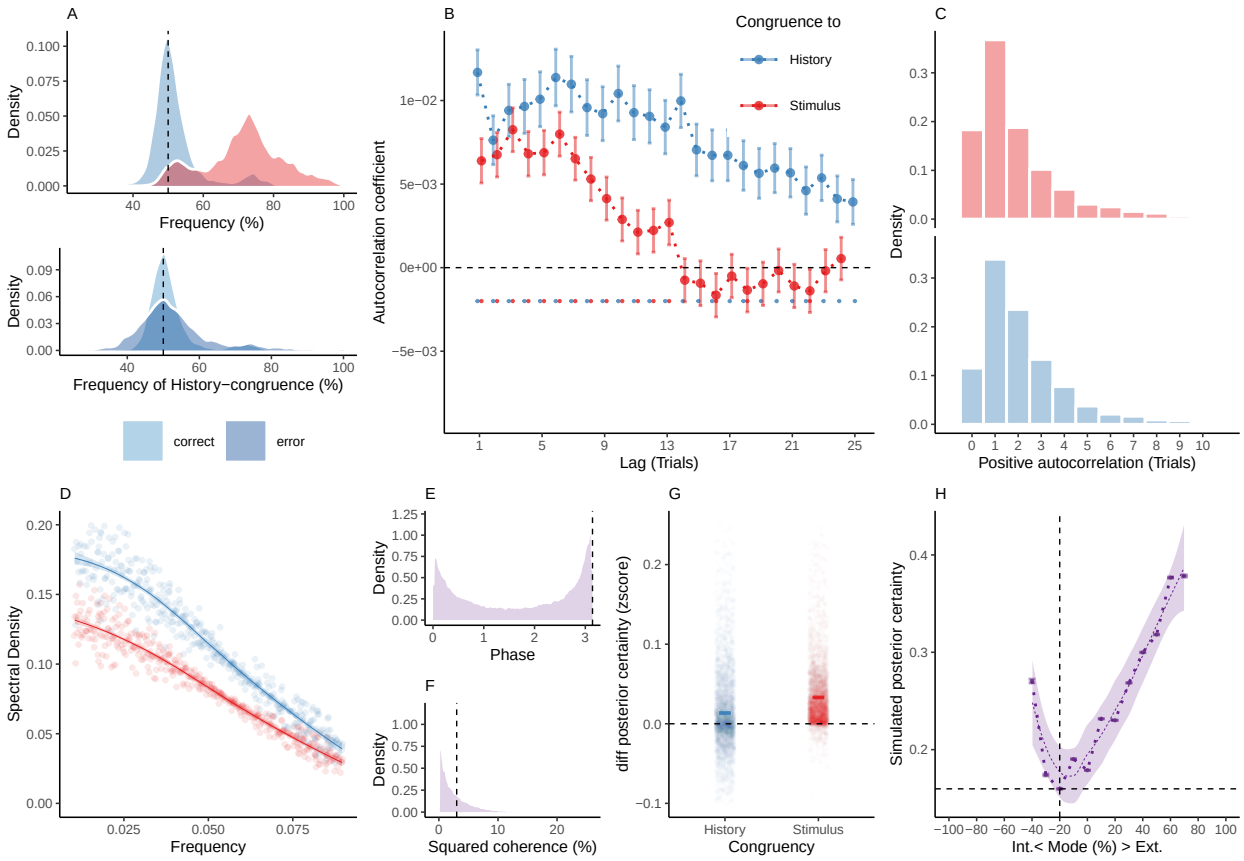

Figure 4. Internal and external modes in simulated perceptual decision-making.

A. Simulated perceptual choices were stimulus-congruent in 71.36% ± 0.17% (in red) and history-congruent in 51.99% ± 0.11% of trials (in blue; $T(4.32 \times 10^3) = 17.42$, $p = 9.89 \times 10^{-66}$; upper panel). Due to the competition between stimulus- and history-congruence, history-congruent perceptual choices were more frequent when perception was stimulus-incongruent (i.e., on *error* trials; $T(4.32 \times 10^3) = 11.19$, $p = 1.17 \times 10^{-28}$; lower panel) and thus impaired performance in the randomized psychophysical design simulated here.

B. At the simulated group level, we found significant autocorrelations in both stimulus-congruence (13 consecutive trials) and history-congruence (30 consecutive trials).

C. On the level of individual simulated participants, autocorrelation coefficients exceeded the autocorrelation coefficients of randomly permuted data within a lag of $2.46 \pm 1.17 \times 10^{-3}$

trials for stimulus-congruence and $4.24 \pm 1.85 \times 10^{-3}$ trials for history-congruence.

D. The smoothed probabilities of stimulus- and history-congruence (sliding windows of ± 5 trials) fluctuated as a scale-invariant process with a 1/f power law, i.e., at power densities that were inversely proportional to the frequency (power $\sim 1/f^{\beta}$; stimulus-congruence: $\beta = -0.81 \pm 1.18 \times 10^{-3}$, $T(1.92 \times 10^5) = -687.58$, $p < 2.2 \times 10^{-308}$; history-congruence: $\beta = -0.83 \pm 1.27 \times 10^{-3}$, $T(1.92 \times 10^5) = -652.11$, $p < 2.2 \times 10^{-308}$).

E. The distribution of phase shift between fluctuations in simulated stimulus- and history-congruence peaked at half a cycle (π denoted by dotted line). The dynamic probabilities of simulated stimulus- and history-congruence were therefore were strongly anti-correlated ($\beta = -0.03 \pm 8.22 \times 10^{-4}$, $T(2.12 \times 10^6) = -40.52$, $p < 2.2 \times 10^{-308}$).

F. The average squared coherence between fluctuations in simulated stimulus- and history-congruence (black dotted line) amounted to $6.49 \pm 2.07 \times 10^{-3}\%$.

G. Simulated confidence was enhanced for stimulus-congruence ($\beta = 0.03 \pm 1.71 \times 10^{-4}$, $T(2.03 \times 10^6) = 178.39$, $p < 2.2 \times 10^{-308}$) and history-congruence ($\beta = 0.01 \pm 1.5 \times 10^{-4}$, $T(2.03 \times 10^6) = 74.18$, $p < 2.2 \times 10^{-308}$).

H. In analogy to humans, the simulated data showed a quadratic relationship between the mode of perceptual processing and posterior certainty, which increased for stronger external and internal biases ($\beta_2 = 31.03 \pm 0.15$, $T(2.04 \times 10^6) = 205.95$, $p < 2.2 \times 10^{-308}$). The horizontal and vertical dotted lines indicate minimum posterior certainty and the associated mode, respectively.

References

1. Schrödinger, E. *What is life? The physical aspect of the living cell.* (Cambridge University Press, 1944).

2. Ashby, W. R. Principles of the self-organizing dynamic system. *Journal of General Psychology* **37**, 125–128 (1947).

3. Friston, K. *et al.* The anatomy of choice: Active inference and agency. *Frontiers in human neuroscience* **7**, 598 (2013).

4. Palva, J. M. *et al.* Roles of multiscale brain activity fluctuations in shaping the variability and dynamics of psychophysical performance. in *Progress in Brain Research* vol. 193 335–350 (Elsevier B.V., 2011).

5. VanRullen, R. Perceptual cycles. *Trends in Cognitive Sciences* **20**, 723–735 (2016).

6. Verplanck, W. *et al.* Nonindependence of successive responses in measurements of the visual threshold. *psycnet.apa.org* (1952).

7. Atkinson, R. C. A variable sensitivity theory of signal detection. *Psychological Review* **70**, 91–106 (1963).

8. Dehaene, S. Temporal oscillations in human perception. *Psychological Science* **4**, 264–270 (1993).

9. Gilden, D. L. *et al.* On the nature of streaks in signal detection. *Cognitive Psychology* **28**, 17–64 (1995).

10. Gilden, D. L. *et al.* 1/f noise in human cognition. *Science* **67**, 1837–1839 (1995).

11. Monto, S. *et al.* Very slow EEG fluctuations predict the dynamics of stimulus detection and oscillation amplitudes in humans. *Journal of Neuroscience* **28**, 8268–8272 (2008).

12. Ashwood, Z. C. *et al.* Mice alternate between discrete strategies during perceptual decision-making. *Nature Neuroscience* **25**, 201–212 (2022).

13. Gilden, D. L. Cognitive emissions of 1/f noise. *Psychological Review* **108**, 33–56 (2001).

14. Duncan, K. *et al.* Memory's penumbra: Episodic memory decisions induce lingering mnemonic biases. *Science* **337**, 485–487 (2012).

15. Kelly, A. M. C. *et al.* Competition between functional brain networks mediates behavioral variability. *NeuroImage* **39**, 527–537 (2008).

16. Hesselmann, G. *et al.* Spontaneous local variations in ongoing neural activity bias perceptual decisions. *Proceedings of the National Academy of Sciences of the United States of America* **105**, 10984–10989 (2008).

17. Schroeder, C. E. *et al.* Dynamics of active sensing and perceptual selection. *Current Opinion in Neurobiology* **20**, 172–176 (2010).

18. Honey, C. J. *et al.* Switching between internal and external modes: A multiscale learning principle. *Network Neuroscience* **1**, 339–356 (2017).

19. Weilnhammer, V. *et al.* Bistable perception alternates between internal and external modes of sensory processing. *iScience* **24**, (2021).

20. Rahnev, D. *et al.* The confidence database. *Nature Human Behaviour* **4**, 317–325 (2020).

21. Aguillon-Rodriguez, V. *et al.* Standardized and reproducible measurement of decision-making in mice. *eLife* **10**, (2021).

22. Fischer, J. *et al.* Serial dependence in visual perception. *Nat. Neurosci.* **17**, 738–743 (2014).

23. Liberman, A. *et al.* Serial dependence in the perception of faces. *Current Biology* **24**, 2569–2574 (2014).

24. Abrahamyan, A. *et al.* Adaptable history biases in human perceptual decisions. *Proceedings of the National Academy of Sciences of the United States of America* **113**, E3548–E3557 (2016).

25. Cicchini, G. M. *et al.* Compressive mapping of number to space reflects dynamic encoding mechanisms, not static logarithmic transform. *Proceedings of the National Academy of Sciences of the United States of America* **111**, 7867–7872 (2014).

26. Cicchini, G. M. *et al.* Serial dependencies act directly on perception. *Journal of Vision* **17**, (2017).

27. Fritsche, M. *et al.* A bayesian and efficient observer model explains concurrent attractive and repulsive history biases in visual perception. *eLife* **9**, 1–32 (2020).

28. Urai, A. E. *et al.* Pupil-linked arousal is driven by decision uncertainty and alters serial choice bias. *Nature Communications* **8**, (2017).

29. Akrami, A. *et al.* Posterior parietal cortex represents sensory history and mediates its effects on behaviour. *Nature* **554**, 368–372 (2018).

30. Braun, A. *et al.* Adaptive history biases result from confidence-weighted accumulation of past choices. *Journal of Neuroscience* **38**, 2418–2429 (2018).

31. Bergen, R. S. V. *et al.* Probabilistic representation in human visual cortex reflects uncertainty in serial decisions. *Journal of Neuroscience* **39**, 8164–8176 (2019).

32. Urai, A. E. *et al.* Choice history biases subsequent evidence accumulation. *eLife* **8**, (2019).

33. Hsu, S. M. *et al.* The roles of preceding stimuli and preceding responses on assimilative and contrastive sequential effects during facial expression perception. *Cognition and Emotion* **34**, 890–905 (2020).

34. Dong, D. W. *et al.* Statistics of natural time-varying images. *Network: Computation in Neural Systems* **6**, 345–358 (1995).

35. Burr, D. *et al.* Vision: Efficient adaptive coding. *Current Biology* vol. 24 R1096–R1098 (2014).

36. Montroll, E. W. *et al.* On 1/f noise and other distributions with long tails. *Proceedings of the National Academy of Sciences* **79**, 3380–3383 (1982).

37. Bak, P. *et al.* Self-organized criticality: An explanation of the 1/f noise. *Physical Review Letters* **59**, 381–384 (1987).

38. Chialvo, D. R. Emergent complex neural dynamics. *Nature Physics* **6**, 744–750 (2010).

39. Wagenmakers, E. J. *et al.* Estimation and interpretation of 1/f noise in human cognition. *Psychonomic Bulletin and Review* **11**, 579–615 (2004).

40. Orden, G. C. V. *et al.* Human cognition and 1/f scaling. *Journal of Experimental Psychology: General* **134**, 117–123 (2005).

41. Chopin, A. *et al.* Predictive properties of visual adaptation. *Current Biology* **22**, 622–626 (2012).

42. Cicchini, G. M. *et al.* The functional role of serial dependence. *Proceedings of the Royal Society B: Biological Sciences* **285**, (2018).

43. Kiyonaga, A. *et al.* Serial dependence across perception, attention, and memory. *Trends in Cognitive Sciences* **21**, 493–497 (2017).

44. Kepecs, A. *et al.* Neural correlates, computation and behavioural impact of decision confidence. *Nature* **455**, 227–231 (2008).

45. Fleming, S. M. *et al.* How to measure metacognition. *Frontiers in Human Neuroscience* **8**, 443 (2014).

46. John-Saaltink, E. St. *et al.* Serial dependence in perceptual decisions is reflected in activity patterns in primary visual cortex. *Journal of Neuroscience* **36**, 6186–6192 (2016).

47. Cicchini, G. M. *et al.* Perceptual history propagates down to early levels of sensory analysis. *Current Biology* **31**, 1245–1250.e2 (2021).

48. Akaike, H. Factor analysis and AIC. *Psychometrika* **52**, 317–332 (1987).

49. Leys, C. *et al.* Detecting outliers: Do not use standard deviation around the mean, use absolute deviation around the median. *Journal of Experimental Social Psychology* **49**, 764–766 (2013).

50. Maloney, L. T. *et al.* Past trials influence perception of ambiguous motion quartets through pattern completion. *Proceedings of the National Academy of Sciences of the United States of America* **102**, 3164–3169 (2005).

51. Glaze, C. M. *et al.* Normative evidence accumulation in unpredictable environments. *eLife* **4**, (2015).

52. Wexler, M. *et al.* Persistent states in vision break universality and time invariance. *Proceedings of the National Academy of Sciences of the United States of America* **112**, 14990–14995 (2015).

53. Feldman, H. *et al.* Attention, uncertainty, and free-energy. *Frontiers in Human Neuroscience* **4**, 7028 (2010).

54. Mathys, C. D. *et al.* Uncertainty in perception and the hierarchical gaussian filter. *Frontiers in human neuroscience* **8**, 825 (2014).

55. Friston, K. A theory of cortical responses. *Philosophical transactions of the Royal Society of London. Series B, Biological sciences* **360**, 815–836 (2005).

56. Sterzer, P. *et al.* The predictive coding account of psychosis. *Biological Psychiatry* **84**, 634–643 (2018).

57. Jardri, R. *et al.* Experimental evidence for circular inference in schizophrenia. *Nature Communications* **8**, 14218 (2017).

58. Bengio, Y. *et al.* Towards biologically plausible deep learning. *bioRxiv* (2015).

59. Dijkstra, N. *et al.* Perceptual reality monitoring: Neural mechanisms dissociating imagination from reality. *PsyArXiv* (2021) doi:10.31234/OSF.IO/ZNGEQ.

60. Bitzer, S. *et al.* Perceptual decision making: Drift-diffusion model is equivalent to a bayesian model. *Frontiers in Human Neuroscience* **8**, 77624 (2014).

61. Roy, N. A. *et al.* Extracting the dynamics of behavior in sensory decision-making experiments. *Neuron* **109**, 597–610.e6 (2021).

62. Ashwood, Z. C. *et al.* Mice alternate between discrete strategies during perceptual decision-making. *bioRxiv* 2020.10.19.346353 (2021) doi:10.1101/2020.10.19.346353.

63. Matthews, G. *et al.* Task engagement, attention, and executive control. 205–230 (2010) doi:10.1007/978-1-4419-1210-7_13.

64. McGinley, M. J. *et al.* Waking state: Rapid variations modulate neural and behavioral responses. *Neuron* **87**, 1143–1161 (2015).

65. Beerendonk, L. *et al.* A disinhibitory circuit mechanism explains a general principle of peak performance during mid-level arousal. *bioRxiv* 2023.07.28.550956 (2023) doi:10.1101/2023.07.28.550956.

66. Gee, J. W. D. *et al.* Decision-related pupil dilation reflects upcoming choice and individual bias. *Proceedings of the National Academy of Sciences of the United States of America* **111**, E618–E625 (2014).

67. Gee, J. W. de *et al.* Dynamic modulation of decision biases by brainstem arousal systems. *eLife* **6**, (2017).

68. Gee, J. W. de *et al.* Pupil-linked phasic arousal predicts a reduction of choice bias across species and decision domains. *eLife* **9**, 1–25 (2020).

69. McGinley, M. J. *et al.* Waking state: Rapid variations modulate neural and behavioral responses. *Neuron* **87**, 1143–1161 (2015).

70. Gee, J. W. de *et al.* Mice regulate their attentional intensity and arousal to exploit increases in task utility. *bioRxiv* 2022.03.04.482962 (2022) doi:10.1101/2022.03.04.482962.

71. Laboratory, I. B. *et al.* A brain-wide map of neural activity during complex behaviour. doi:10.1101/2023.07.04.547681.

72. Mawase, F. *et al.* Movement repetition facilitates response preparation. *Cell reports* **24**, 801–808 (2018).

73. Pomper, U. *et al.* Motor-induced oscillations in choice response performance. *Psychophysiology* **60**, e14172 (2023).

74. Kepecs, A. *et al.* A computational framework for the study of confidence in humans and animals. *Philosophical Transactions of the Royal Society B: Biological Sciences* **367**, 1322 (2012).

75. Fritsche, M. *et al.* Opposite effects of recent history on perception and decision. *Current Biology* **27**, 590–595 (2017).

76. Gekas, N. *et al.* Disambiguating serial effects of multiple timescales. *Journal of Vision* **19**, 1–14 (2019).

77. Weilnhammer, V. *et al.* Psychotic experiences in schizophrenia and sensitivity to sensory evidence. *Schizophrenia bulletin* **46**, 927–936 (2020).

78. Fletcher, P. C. *et al.* Perceiving is believing: A bayesian approach to explaining the positive symptoms of schizophrenia. *Nature reviews. Neuroscience* **10**, 48–58 (2009).

79. Corlett, P. R. *et al.* Hallucinations and strong priors. *Tics* **23**, 114–127 (2019).

80. Nash, J. C. *et al.* Unifying optimization algorithms to aid software system users: Optimx for r. *Journal of Statistical Software* **43**, 1–14 (2011).

81. Findling, C. *et al.* Brain-wide representations of prior information in mouse decision-making. *bioRxiv* 2023.07.04.547684 (2023) doi:10.1101/2023.07.04.547684.

82. Feigin, H. *et al.* Perceptual decisions are biased toward relevant prior choices. *Scientific Reports 2021 11:1* **11**, 1–16 (2021).

Supplemental Information

- Supplement_clean.pdf: Supplemental Items and Figures
- Supplement_track_changes.pdf : Supplemental Items and Figures

The above files contain the following supplemental items and figures:

Supplemental Text Items

1. Internal mode processing is driven by choice history as opposed to stimulus history
2. Internal mode is characterized by lower thresholds as well as by history-dependent changes in biases and lapses
3. Internal mode processing can not be reduced to insufficient task familiarity

Supplemental Figures

1. Supplemental Figure S1. Stimulus- and history-congruence.
2. Supplemental Figure S2. Controlling for task difficulty and external stimulation
3. Supplemental Figure S3. Reproducing group-level autocorrelations using logistic regression
4. Supplemental Figure S4. History-congruence in logistic regression.
5. Supplemental Figure S5. Correcting for general response biases
6. Supplemental Figure S6. Full and history-conditioned psychometric functions across modes in humans
7. Supplemental Figure S7. Full and history-conditioned psychometric functions across modes in mice

8. Supplemental Figure S8. History-/stimulus-congruence and TDs during training of the basic task

9. Supplemental Figure S9. Comparison of the bimodal inference model against reduced control models

10. Supplemental Figure S10. Reduced Control Model M2: Only oscillation of the likelihood

11. Supplemental Figure S11. Reduced Control Model M3: Only oscillation of the prior

12. Supplemental Figure S12. Reduced Control Model M4: Normative evidence accumulation

13. Supplemental Figure S13. Reduced Control Model M5: No accumulation of information across trials.

14. Supplemental Figure S14. Autocorrelation of history-congruence of alternating and repeating biases

Supplemental Tables

1. Supplemental Table T1. Studies extracted from the Confidence Database

2. Supplemental Table T2. Explanation of model parameters